International Journal of Pharmaceutics 668 (2025) 124978

Contents lists available at ScienceDirect

International Journal of Pharmaceutics

journal homepage: www.elsevier.com/locate/ijpharm

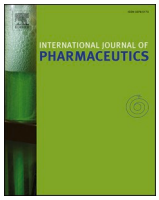

Hyaluronan-Cholesterol nanogels embedding betamethasone for the treatment of skin inflammatory conditions

Ju Wang [a,b], Daniel Di Risola [c], Roberto Mattioli [c], Nicole Zoratto [a], Luciana Mosca [c], Chiara Di Meo [a], Pietro Matricardi [a,*]

[a] Departments of Drug Chemistry and Technologies, Sapienza University of Rome, P.le Aldo Moro 5, Rome 00185, Italy
[b] The Academy of Chinese Health Risks, West China Hospital, Sichuan University, No. 37 Guoxue Road, Chengdu 610041, China
[c] Department of Biochemical Sciences "A. Rossi Fanelli", Sapienza University of Rome, P.le Aldo Moro 5, Rome 00185, Italy

ARTICLE INFO

Keywords:
Hyaluronan-Cholesterol
Nanogels
Skin permeation
Psoriasis
Betamethasone

ABSTRACT

Topical application of the glucocorticoid betamethasone (BM) is a common treatment for inflammatory-related skin diseases, such as psoriasis. However, enhancing its bioavailability remains challenging due to poor skin permeability. Herein, we developed and evaluated hyaluronan-cholesterol (HACH) based nanohydrogel systems (NHs) and NHs-Carbopol formulation for dermal delivery of BM. Various parameters were investigated including particle size, surface charge, encapsulation efficiency, *in vitro* drug release kinetics and stability. The HACH-based NHs demonstrated high encapsulation efficiency, with apparent solubility improved up to 9-fold, small size (~190 nm) and good stability at 4 ℃ and during long-term storage. Besides, the NHs-Carbopol formulation exhibited excellent rheological properties and an occlusive effect suitable for cutaneous application. Both *in-vitro* (using Strat-M® membrane) and *ex-vivo* (using pig ear skin) permeation studies revealed that these formulations significantly improved skin permeation and drug retention in the deeper layers of the epidermis and dermis, making it advantageous for the topical delivery of BM in psoriasis treatment. Moreover, the NHs system demonstrated potential anti-psoriatic activity by downregulating the proinflammatory cytokines *in vitro* in human keratinocytes (HaCaT cell line) and in an *ex vivo* 3D skin tissue model (EpiDerm-FT™).

1. Introduction

Psoriasis is a chronic inflammatory skin disease that affects approximately 2–4 % of the global population, significantly impacting their quality of life and psychological well-being (Parisi et al., 2020). It is typically characterized by thickened plaques owing to the hyper-proliferation and incomplete differentiation of epidermal keratinocytes. The pathogenesis of psoriasis is complex and multifactorial, involving genetic predisposition, immune system dysregulation, and environmental triggers (Coda et al., 2012; Lowes et al., 2014). Patients with psoriasis experience relapsing episodes of inflammatory skin lesions, accompanied by endothelial vascular changes in the dermal layer, such as angiogenesis, blood vessel dilation, and high endothelial venule (HEV) formation, which are driven by various inflammatory cytokines released in the inflammatory process (Ayala-Fontánez et al., 2016; Rendon and Schäkel, 2019). Management of psoriasis includes a range of treatments such as topical therapy, phototherapy, and systemic therapy (oral medications or injections). However, none of these approaches offers a complete cure. In severe cases, traditional systemic drug administration is employed but often leads to significant adverse. Moreover, new biological treatments have emerged for severe psoriasis, but comprehensive data on their long-term efficacy and safety are still limited, and not every patient effectively responds to these therapies (Armstrong et al., 2015; Sawyer et al., 2015). For milder cases, topical therapy is commonly preferred due to its minimal systemic exposure and fewer side effects.

Among the various treatment options, the topical use of glucocorticoids, specifically betamethasone (BM), is widely favored for psoriasis management. BM, a highly potent glucocorticoid receptor agonist, is renowned for its immunosuppressive, anti-inflammatory, and anti-proliferative properties. Various formulations of BM, such as ointments, creams, foams, and gels, have been developed and utilized for treating mild to moderate psoriasis (Shalaby et al., 2022). However, there are some practical drawbacks in the clinical application of BM. Its poor solubility and limited permeability through the skin barrier, coupled with burst release from conventional formulations, contribute

* Corresponding author at: Departments of Drug Chemistry and Technologies, Sapienza University of Rome, Piazzale Aldo Moro 5, Rome 00185, Italy.
E-mail address: pietro.matricardi@uniroma1.it (P. Matricardi).

https://doi.org/10.1016/j.ijpharm.2024.124978
Received 30 September 2024; Received in revised form 16 November 2024; Accepted 18 November 2024
Available online 20 November 2024

to poor bioavailability, reduced therapeutic efficacy, and potential systemic toxicity (Dhar et al., 2014). Therefore, a major challenge in topical formulation lies in enhancing the drug's penetration through the skin, particularly the thickened stratum corneum characteristic of psoriasis, without causing any significant and irreversible alteration to the skin barrier function (Baboota et al., 2011).

Hydrogels have emerged as potent vehicles for topical drug delivery due to their distinctive attributes, including high water content and versatile viscoelastic behavior. Unlike creams and ointments, hydrogel-based formulations consist of non-greasy ingredients that self-assemble into a three-dimensional network structure. This structure provides a cooling effect due to surface evaporation and sustains skin hydration, consequently reducing *trans*-epidermal water loss. Hydrogels exhibit unique characteristics in drug delivery, influenced by factors such as mesh size, degradation rate of the hydrogel, and interactions between the drug and hydrogel network (Du et al., 2015; Li et al., 2012; Lombardo et al., 2015). Nanotechnology-based drug delivery has garnered considerable interest within the pharmaceutical field, offering a captivating avenue for encapsulating and delivering therapeutic agents. Nanogels combine the advantages of both hydrogels and nanoscale drug carriers, facilitating efficient drug loading and enhanced penetration into target tissues (Vincent et al., 2014). A wide variety of gels have been reported, encompassing both covalent and non-covalent crosslinking approaches, with widespread applications across various biomedical domains, notably drug delivery. Polymers with natural and synthetic properties have been developed as drug carriers to improve topical skin delivery (Filippone et al., 2020; Jebbawi et al., 2020b; Panonnummal et al., 2017; Panonnummal and Sabitha, 2018). Nanogels, crafted from natural polymers like polysaccharides, present an additional advantage owing to their inherent biocompatibility and biodegradability.

Hyaluronic acid (HA), also known as hyaluronan, is a natural polysaccharide composed of repeating units of N-acetyl-D-glucosamine and D-glucuronic acid, linked together *via* alternating β-1,3 and β-1,4 glycosidic bonds. As a non-sulfated, anionic glycosaminoglycan, HA is abundant in the skin and serves as a compelling candidate for nanogel formulation due to its intrinsic gelling properties and capacity for crosslinking or conjugation with other molecules (Bayer, 2020; Fakhari and Berkland, 2013).

Moreover, due to the specific interaction with CD44 receptors, which are abnormally expressed in psoriatic skin, HA-based nanogels can be employed for targeted topical administration (Zhang et al., 2019). Consequently, HA and its derivatives are extensively used, particularly in wound healing, skin infections, and inflammatory skin diseases (Montanari et al., 2020; Zhu et al., 2018). Although HA in its native form exhibits utility, chemical conjugation with lipophilic molecules like cholesterol (CH) can enhance drug encapsulation capacity and facilitate nanogel formation through self-assembly under certain conditions (Montanari et al., 2019; Zoratto et al., 2021a). CH is a biocompatible and naturally occurring molecule in the skin, making it an ideal candidate for hydrophobic grafting onto hydrophilic HA chains (Boer et al., 2020). In our previous work, both hydrophobic and hydrophilic drugs were successfully loaded into self-assembled HA-CH nanogels to enhance ocular drug delivery (Zoratto et al., 2021a).

The primary objective of the present study was to formulate HA-CH-based nanogels for the topical delivery of BM as a promising approach for psoriasis management. To improve the rheological properties of the formulation, BM-loaded nanogels were incorporated into a Carbopol base, known for its impressive mucoadhesive, viscosity and rheological properties. We investigated the characteristics of both nanogels and formulations and evaluated their skin permeation abilities *in vitro* (using an artificially synthesized membrane) and *ex vivo* (in pig ear skin). A comparison with commercial formulations was also conducted. *In vitro* cytotoxicity was assessed on HaCaT cells, whereas anti-inflammatory activity was assayed using full-thickness 3D skin equivalents (EpiDerm-FT™). The long-term goal of this work is to develop a topical BM nanogel formulation suitable for clinical application, thereby enhancing therapeutic efficacy in the management of psoriasis.

2. Materials and methods

2.1. Materials

Hyaluronan tetrabutylammonium salt (HA-TBA$^+$, molecular weight (Mw) = 2.2×10^5) was purchased from Hysilk (Dolní Dobrouc, Czech Republic). Cholesterol (CH), 4-bromobutyric acid, N-methyl-2-pyrrolidone (NMP), N-(3-dimethylaminopropyl)-N'-(ethylcarbodimide hydrochloride) (EDC·HCl), acetone, acetonitrile (HPLC grade), betamethasone, triethanolamine (TEA, purity ≥ 99 %), phosphate buffered saline (PBS) tablets, TRIreagent® and Hanks' balanced salt solution were purchased from Sigma-Aldrich (Milan, Italy). Carbopol® 940 (polyacrylic acid polymer crosslinked with allyl pentaerythritol) was purchased from Farmacisti Associati, Italy. Dialysis tubing cellulose membrane was purchased from Sigma Aldrich. Ecoval® commercial solution (0.5 mg/g), and Diprosone® cream (0.05 %, w/w) were purchased from the local pharmacy. Fresh pig ears were collected from the local slaughterhouse. GoTaq® 2-Step RT-qPCR kit was purchased from Promega®.

2.2. Synthesis of HA-CH

The method for the synthesis of hyaluronan-cholesterol (HA-CH) derivative was already described in detail in previous work (Montanari et al., 2013).

2.3. Preparation of empty and betamethasone (BM) loaded NHs

The BM loaded NHs were prepared using an autoclave process, as previously reported. Briefly, 3.0 mg of HA-CH polymers (degree of functionalisation (Df) = 15 %, mol of CH/mol of HA repeating units) were dispersed in 3.0 mL of distilled water (1 mg/mL) by magnetic stirring overnight at 25 ℃. BM was solubilized in acetone at 3 mg/mL or 4 mg/mL to create a stock solution. A 0.5 mL aliquot of this stock solution was added to a glass vial and evaporated using a rotary evaporator (Buchi, Schwabach, Germany) to form the drug film. This film was then mixed with 3 mL of HA-CH suspension. The mixtures were maintained under magnetic stirring at 25 ℃, with periodic vortex shaking, and then autoclaved (121 °C, 1.1 bar) for 20 min to form BM-NHs.

The samples were subsequently centrifuged at 4000 rpm for 15 min at 25 ℃ (Universal 30RF, Hettich Zentrifugen, Germany). The supernatant containing NHs was stored for further studies, whilst the pellets (unloaded drug) were used to indirectly quantify BM entrapped into NHs. Blank NHs were also prepared following the same protocol without adding BM.

2.4. Quantification of entrapped BM in NHs

To quantify the entrapped BM in NHs, the BM pellets (unloaded drug) were dissolved in acetonitrile. The amount of entrapped drug was then determined indirectly. The analysis was performed using a Knauer Azura HPLC instrument was used for the analysis, which was equipped with a binary pump (Azura P 6.1 L) and a UV–Vis detector (190–750 nm, Azura UVD 2.1 L), controlled by Clarity software. Chromatographic separation was achieved using a Knauer Eurospher II C18 column (4.6 × 250 mm, 5 μm). The mobile phase consisted of acetonitrile: water (50:50, v/v) initially in initial isocratic mode, followed by a gradient mode from 50:50 to 100:0. The flow rate was maintained at 1 mL/min, 20 μL of the sample was loaded for each injection. The analysis were performed at ambient temperature and UV detection at 250 nm. The amount of unloaded BM was quantified using a calibration curve created with BM standard solution in acetonitrile, ranging from 1 to 200 μg/mL ($R^2 = 0.9999$).

Encapsulation efficiency (*EE*) and drug loading (*DL*) were calculated

using the following equations (1) and (2).

$$EE\% = \frac{(Total\ mass\ of\ drug) - (Mass\ of\ untrapped\ drug)}{Total\ mass\ of\ drug} \times 100 \quad (1)$$

$$DL\% = \frac{Concentration\ of\ loaded\ drug\ in\ gel\ sample(\mu g/mL)}{Polymer\ concentration\ in\ gel\ sample(\mu g/mL)} \times 100 \quad (2)$$

2.5. Size and surface charge of NHs

The Z-average size and zeta potential of the NHs were measured at 25 ℃ using a Zetasizer Nano ZS instrument (Model ZEN3690, Malvern Instruments, Worcestershire, UK) equipped with a solid state HeNe laser (λ = 633 nm) at a scattering angle of 173°. Particle average size and polydispersity index (PDI) of the prepared NHs were evaluated by dynamic light scattering (DLS), with detection performed at a refractive index of 1.40. The size of the samples was described in terms of hydrodynamic diameter (Z-average size). The zeta potential (ζ-potential) was calculated from the electrophoretic mobility of the samples using the Smoluchowski equation.

To investigate the stability of BM-NHs, DLS measurements were carried out at 1, 3, 5, 7, 10, and 14 days. For comparison, blank NHs samples were also measured. Samples were stored at 4 ℃ between the measurements, each measurement was performed at ambient temperature and in triplicate (n = 3).

For long-term storage experiments, NHs samples were freeze-dried. Before freezing, a cryoprotectant solution (20 % w/v dextrose in water) was added into NHs suspension (final dextrose concentration of 1 % w/v) and gently stirred overnight at 4 ℃. The freeze-dried product was re-suspended in the same volume of water and vortexed for homogeneity. The re-suspensions were analyzed by DLS to determine size and PDI of the re-formed NHs.

2.6. Preparation of Carbopol-based gel formulation

To prepare the Carbopol-based gel formulation, Carbopol® 940 NF was dispersed at 0.75 % (w/v) in double distilled water by magnetic stirring overnight at ambient conditions to create a Carbopol suspension (with a pH around 3). For each milliliter of the final Carbopol gel volume, 20 μL of TEA (15 %, v/v) was added dropwise under continuous stirring until a homogenous mixture was achieved, with a pH of around 6. Subsequently, 1 mL of Carbopol gel stock (0.75 %, w/v) was diluted with 2 mL of the prepared BM-NHs, and gently stirred with a magnetic stirrer at approximately 90 rpm to obtain BM-NHs-Carbopol gel. The final pH of the Carbopol-based gel was checked to be around 5.6. For the BM-loaded Carbopol gel, BM-loaded NHs (BM-NHs) were prepared by loading 2 mg of BM into 3 mL of the polymer suspension. The final concentration of BM in the gel was approximately 0.43 % (w/w), and the concentration of Carbopol in the gel was 0.25 % (w/v).

2.7. Rheology of Carbopol gel embedding nanogels

The rheological properties of the Carbopol gel incorporating NHs were analyzed using a stress-controlled Discovery Hybrid Rheometer (TA-Instruments, New Castle, Delaware, USA), equipped with a Peltier temperature controlling unit. Measurements were performed at skin surface temperature (32 ℃). The samples were placed in parallel-plate geometry with a 40 mm diameter and a fixed gap of 27 μm. Multiple viscoelastic properties were measured, including viscosity changes with shear rate, variation in viscoelastic modulus and phase angle with shear strain, and complex modulus and complex viscosity with temperature. The linear viscoelastic region (LVR) was determined according to a dynamic amplitude sweep study, with strain percentages increasing from 0.1 % to 100 % at a constant frequency of 1 Hz. Oscillation frequency sweep tests were performed over a frequency range of 0.1 to 10.0 Hz, with a constant amplitude of 1 % strain to remain within the LVR. The viscous modulus (G′), and elastic modulus (G″) were measured. Flow sweep tests were performed with the shear rate ranging from 0.001 s^{-1} to 1000 s^{-1}, and viscosity flow curves as a function of shear rate were constructed.

To mimic the behavior of the formulation during application, a strain recovery test was conducted. Specifically, five cycles of intercalating low (0.1 s^{-1}) and high (100 s^{-1}) shear rates were applied, and the sample's viscosity was continuously monitored. Each test included three low-shear cycles and two high-shear cycles, with durations of 150 s and 30 s per cycle, respectively. Finally, the rheological stability of the gel formulation was assessed by subjecting the sample to temperature ranges from 25 ℃ to 40 ℃ under constant shear and frequency, recording changes in complex viscosity and complex modulus.

Experiments for each condition were repeated three times, and results were obtained using Trios software (V.5.1.1, TA Instruments, New Castle, DE, USA).

2.8. Occlusive tests

The occlusive properties of Carbopol-based gels and NHs were evaluated using an *in vitro* occlusion test according to the procedure reported by Montenegro et al. (Montenegro et al., 2017). Beakers (50 mL) were filled with 25 mL of distilled water, covered with Whatman filter paper and carefully sealed with Teflon tape. Approximately 200 mg of each gel formulation was uniformly spread evenly on the filter surface using a spatula to form a thin film. This application was repeated every 24 h. Beakers containing 25 mL of distilled water, covered with filter paper but without any applied sample, served as the control. All beakers were kept in an oven at 32 ℃ to mimic the skin surface temperature for 48 h. The beakers were weighed at 24 h and 48 h to measure water loss due to evaporation through the filter cover. Each experiment was carried out in triplicate.

The occlusion factor (F) was calculated according to the following equation:

$$F = \frac{A - B}{A} \times 100 \quad (3)$$

where F is the occlusion factor, A is the water loss without the sample (control), and B is the water loss with the sample applied.

2.9. In vitro release studies

The *in vitro* release behavior of BM from different systems was performed using the dialysis method under two pH conditions: 7.4 (physiology) and 5.5 (skin). Briefly, a known amount of BM-NHs (1 mL) or Carbopol-based gel (1 g) was placed in a dialysis bag (molecular weight cutoff between 12,000–14,000 Da), with both ends of the tube securely closed. The dialysis bag was then immersed in 30 mL of release medium (PBS, pH 7.4 or 5.5) in a water bath maintained at 32 ℃ with constant stirring at 100 rpm. The sink conditions were maintained throughout the experiment. At predefined time points, 5 mL of the release medium was withdrawn and immediately replaced with an equal volume of fresh medium. The withdrawn samples were freeze-dried to remove any water or solvent, and the concentration of released BM in the medium was then determined by HPLC with acetonitrile as the solvent. To understand the release mechanism of the NHs system, the data was analyzed using different mathematical models to evaluate the release kinetics with the "DD Solver" software. (Khamanga and Walker, 2012; Waghule et al., 2021).

2.10. In vitro Strat-M® membrane permeation and accumulation studies

The transdermal permeation of BM-loaded formulations was evaluated using vertical Franz diffusion cells, which consist of a donor and a receptor compartment separated by a membrane (Bartosova and Bajgar, 2012). The Strat-M® membrane (25 mm, Merck Millipore, Billerica, MA,

USA), a synthetic membrane suitable for predicting human skin diffusion, was employed to investigate the transdermal diffusion of BM from the formulations (Haq et al., 2018a). The effective diffusion area of the diffusion cells was 0.64 cm^2. The membrane was sandwiched between the donor and receiver compartments of the Franz diffusion cells, with the shiny layer facing upward. The donor and receptor compartments were initially filled with 1 mL and 5 mL of PBS buffer (pH 5.5), respectively. After 10 min, the PBS was removed from the donor chamber and replaced with 1 mL of NHs sample or 1 g of formulation, then carefully sealed with parafilm to prevent solvent evaporation. At scheduled time points (2, 6 and 24 h), 1 mL samples were withdrawn from the receptor chamber and immediately replaced with 1 mL of fresh medium to maintain a constant volume. Experiments were performed at 32 ℃ in a water bath with constant stirring of the receptor solution using a magnetic bead at 300 rpm.

Each sample was freeze-dried, and the drug was extracted in 1 mL of acetonitrile, then centrifuged (3000 rpm, 25 ℃) for 3 min to separate insoluble salt. The supernatant was injected into an HPLC to quantify the amount of drug permeated through the membrane. Furthermore, the permeation parameters, including drug fluxes (J), permeability coefficients (K_P) and retention coefficients (K_R), were calculated using the following equations:

$$J_{ss} = \frac{Q_p}{\mathrm{A} \times \mathrm{t}} (\mu g\, cm^{-2}\, h^{-1}) \quad (4)$$

$$J_{RR} = \frac{Q_r}{\mathrm{A} \times \mathrm{t}} (\mu g\, cm^{-2}\, h^{-1}) \quad (5)$$

$$K_P = \frac{J_{SS}}{C_0} (cm\, h^{-1}) \quad (6)$$

$$K_R = \frac{J_{RR}}{C_0} (cm\, h^{-1}) \quad (7)$$

Where Q is the amount of drug permeated across the membrane (Q_p) or retained in the membrane (Q_r); A is the active area available for permeation (0.64 cm^2); C_0 is the initial drug concentration in the formulation, and t is the permeation time.

After completing the penetration experiment, the Strat-M® membrane was removed from the Franz cell and washed three times with 5 mL of PBS, as much free drug as possible from its surface. The membrane was cut into small pieces, and the drug retained inside the membrane was extracted with 3 mL of acetonitrile under magnetic stirring overnight at 4 ℃. Samples were centrifuged at 4000 rpm for 10 min, and the supernatant was measured using HPLC.

2.11. Ex-vivo skin permeation and deposition studies

The *ex-vivo* permeation studies were conducted using isolated pig ear skin (Kaur et al., 2017), by vertical Franz diffusion cells with an effective diffusion area of 0.64 cm^2. These studies aimed to investigate the rate of drug transport across the skin and to determine the drug localized inside the skin layers.

2.11.1. Preparation of porcine skin

Porcine ears were collected from a local slaughterhouse and transported to the laboratory in iced Hanks balanced salt solution (HBSS) (Lau et al., 2012). Pig ears were cleaned using running tap water, and any remaining hairs were removed with surgical blades. Skin samples were collected from the inner part of the pig ears, and the epidermis with dermal layers were separated from the underlying cartilage using a scalpel. The hypodermis, including blood vessels and subcutaneous fat layer, was carefully removed. The isolated integral skin samples were then cut into 2 × 2 cm^2 pieces and dipped in normal buffer saline.

2.11.2. Permeation study

The same Franz diffusion cell setup used for the *in-vitro* diffusion study was adopted for the *ex-vivo* skin permeation studies. The skin sample was mounted on the diffusion cells, with the stratum corneum side facing up, between the donor and receiver compartments. The skin permeation properties of BM-NHs, Carbopol-based formulations (BM-NHs-Carbopol gels) and a commercial formulation (Ecoval solution, GSK) were evaluated. All other conditions were the same as those used in the *in vitro* permeation study.

2.11.3. Skin retention study

After the *ex-vivo* permeation experiments, the remaining sample in the donor compartment was carefully removed with a pipettor or spatula and analyzed for drug quantification using HPLC. The skin tissue mounted on the diffusion cell was carefully isolated, washed the surface three times with PBS solution, and dried with filter paper. Further, the stratum corneum (or visible epidermis) and dermis were then separated using a scalpel from the effective permeation part of the skin (weighted in advance). These samples were suspended in 3 mL of acetonitrile and stirred at 4 ℃ for 24 h with intermittent sonication using a sonicator bath to extract the drug from the skin. The sample was then centrifuged (3000 rpm, 25 ℃, 10 mins), and the obtained supernatant was analyzed using HPLC.

2.12. Cell and EpiDermFT™ skin model culture

Human epidermal keratinocytes (HaCaT) were used to assess the cell toxicity and effects of the NHs system. HaCaT cell line (RRID: CVCL_0038) was cultured in Dulbecco's modified Eagles Medium (DMEM) high glucose medium, supplemented with 10 % fetal bovine serum (FBS), 2 mM L-glutamine, 1 % penicillin–streptomycin solution and kept in an incubator maintained at 37 °C, 5 % of CO_2, and 99 % RH. All the experiments were performed between the 15-25th cell passage.

The *in vitro* skin model, EpiDerm-FT™, is a full-thickness 3D skin equivalent containing normal human epidermal keratinocytes and dermal fibroblasts (EpiDerm-FT™, MatTek In Vitro Life Science Laboratories, s.r.o., Slovakia). The culture medium for EpiDerm-FT in the supernatant (apical medium) and subnatant (basolateral medium) was changed as described in the manufacturer's instructions, and the tissues were maintained under standard conditions (5) % CO_2; 37 °C).

2.13. In vitro cell viability assay

HaCaT cells were used to assess the cell toxicity of the NHs system by MTT 3-(4,5-dimethylthiazol-2-yl)-2,5-diphenyltetrazolium bromide assay. For the cell viability experiments, 96-well plates were seeded with HaCaT cells at a density of 10,000 cells per well. After 24 h, the cells were treated with 1, 10, or 100 μg/mL of NHs (empty and drug-loaded with 0.33 mg/mL of BM) solubilized in sterile bi-distilled water, and 0.33, 3.3 or 33 μg/mL of betamethasone solubilized in DMSO, in a final volume of 150 μL per well. Following a 24-hour incubation period, 20 μL of MTT (5 mg/mL of stock solution in PBS) was added to each well and incubated for an additional 2 h at 37 °C with 5 % CO_2. Water-insoluble formazan crystals were dissolved in 100 μl of DMSO. Appliscan® plate reader (Thermo Scientific) was used for spectrophotometric measurements at the wavelength of 570 nm, with a reference set at 690 nm. The experiments were conducted at least three times. Untreated cells served as the normalizing factor (100 %). In each experiment, control cells were treated with DMSO and water corresponding to the highest concentrations of BM and NHs.

2.14. Evaluation of NHs system biological effects

The NHs system has been tested on both HaCaT cells and EpiDerm-FT™ 3D skin model. HaCaT cells were seeded in 6-well plates at the density of 300′000 cells per well. After 24 h, the cells were starved by

changing the FBS content in the medium from 10 % to 2 %. After 6 h of starvation, the cells were treated with 200 ng/ml of IFN-γ. 24 h later they were treated with 1 μg/mL of NHs (empty and drug-loaded), 0.3 μg/mL of BM or the corresponding volume of DMSO. Non-stimulated cells were treated with DMSO as a control.

Regarding the EpiDerm-FT™ 3D skin model, to induce inflammation, IFN-γ was added to the basolateral medium at a final concentration of 200 ng/mL. After 2 h of incubation, the supernatant was completely replaced with 150 μL of either 1 mg/mL empty NHs solution, BM-NHs, or 300 μg/mL of free BM solution (solubilized in DMSO and diluted with medium, 1.6 % V/V, in medium), applied on the top of the tissue. As the control group, 150 μL of DMSO (1.6 % V/V, in medium) was used. After 24 h of incubation, the tissues were extracted from the transwell and stored at −80 °C for further molecular biology. Non-stimulated cells were treated with DMSO as described before.

HaCaT cells were analyzed, by qRT-PCR, for gene expression of IL-25, IL-33, LORICRIN (LOR), FILAGGRIN (FLG). In similar way, the EpiDerm-FT™ 3D skin model was analyzed for gene expression of IL-25, IL-33, IL-37, IL-10, LORICRIN (LOR), FILAGGRIN (FLG), CD44s, CD44v6 and TNF-α. For qPCR analysis, the tissues were dissected and pottered until completely disrupted in TRI-reagent®. Then, RNA extraction was performed according to the manufacturer's protocol, and the mRNA was quantified and *retro*-transcribed in cDNA, using Promega® GoTaq® 2-Step RT-qPCR kit. qPCR was then performed on a CFX device (BIORAD®) using the SYBR Green fluorescent stain, human *Ribosomal Protein S27A* (*RPS27A*) gene as normalizer and ΔΔCt method to calculate the relative gene expression. The melting curves have been used in order to verify the presence of a single PCR product.

2.15. Statistical analyses

The software OriginPro (Northampton, MA, USA, version 9.1) was used to analyse the data concerning the chemical results. All the results are presented as mean ± standard deviation (SD). The analysis of statistical significance was performed using one-way analysis of variance (ANOVA), followed by Tukey's multiple comparisons. The level of significance was set at $P < 0.05$.

The software Prism® was used to analyse the data concerning the biological results. All the results are presented as mean ± standard error of mean (SEM). The analysis of statistical significance was performed using Brown-Forsythe and Welch ANOVA test and followed by unpaired t with Welch's correction with multiple comparisons. The level of significance was set at $P < 0.05$.

3. Results

One of the major challenges in topical dermal drug delivery is improving the loading efficiency and skin permeability of hydrophobic drugs, especially under conditions like psoriasis where the skin barrier is dysregulated. Psoriasis is associated with alterations in the skin barrier from the early stages of the disease (Visconti et al., 2015). These alterations result from dysregulated processes such as keratinocyte proliferation, tight junction function, and changes in the extracellular matrix (ECM) of the stratum corneum (Orsmond et al., 2021). Consequently, psoriasis is characterized by the formation of psoriatic lesions that exhibit epidermal structural damage, excessive inflammation, and thickened stratum corneum (hyperkeratosis) as well as other epidermal layers (acanthosis) (Orsmond et al., 2021). Hence, innovative topical delivery strategies are required to improve therapeutic bioavailability.

3.1. Preparation and characterization of BM-loaded NHs

Betamethasone (BM), a glucocorticoid drug with strong anti-inflammatory effects but poor water solubility, was loaded into NHs to enhance its solubility and transdermal permeability, thereby achieving high therapeutic efficiency. Different initial amounts of BM were adopted in a fixed volume (3 mL) of HA-CH polymer suspension to investigate the drug loading capacity. The obtained BM-NHs were purified from free drugs through mild centrifugation (4000 rpm for 15 min). The results indicated high encapsulation efficiency (EE%) and hence drug loading (DL%) for all NHs formulations, although the values slightly decreased with an increase in the initial amount of drug. As shown in Fig. 1, DL% values were 31.8 ± 1.1 %, 46.7 ± 2.4 % and 59.6 ± 2.2 % for the different initial amounts of BM, respectively, with all the EE% values exceeding 92 %. This corresponded to NHs drug concentrations of 318, 467 and 596 μg/mL, respectively. Given the water solubility of BM being 66.5 μg/mL, due to the encapsulation into NHs, its apparent water solubility increased by 4.8 to 9.0-fold.

The high DL% and EE% values obtained for BM-NHs can be attributed to hydrophobic interactions between the cholesterol moieties of HA-CH and the hydrophobic drug, promoted by the autoclave process. All drug-loaded NHs were characterized in terms of size, PDI and zeta-potential. The results indicated an average size of approximately 190 nm for drug loaded NHs, similar to that of empty NHs. Besides, the zeta-potential net values for drug-loaded NHs (|-36.5 ± 5.9| mV) were similar to those of empty NHs (|-37.7 ± 0.9| mV), ensuring good stability of the nanoformulations. Furthermore, no significant differences were observed in the size and PDI values of all the samples stored at 4 °C for at least 14 days. The long-term storage stability of drug loaded NHs was also evaluated after the freeze-drying process (Fig. S1). The size and PDI of BM-NHs suspensions, with or without 1 % w/v of dextrose, remained almost the same; however, the re-suspended BM-NHs showed an approximate 20 nm increase in size compared to those before freeze-drying.

3.2. Preparation and characterization of Carbopol-Based gel formulation

HA-CH NHs were incorporated into the Carbopol® 940 gel matrix to create a gel formulation for the topical delivery of BM (Fig. 2). Carbopol, supplied as a white power, is composed of a crosslinked polyacrylic acid polymer. During the preparation of the Carbopol suspension (0.75 %, w/v), a specified quantity of polymer was combined with water and stirred at room temperature overnight, resulting in a pH of around 3 due to the liberation of hydrogen atoms from the carboxylic groups in the polymer structure. The neutralization process involved the gradual addition of TEA (5 %, v/v) while maintaining continuous stirring, aimed to adjust the pH to around 6. During this process, the free hydrogen cations were replaced with the ammonium cation, leading to the swelling of the polymer structure due to the repulsion of negative charges on the carboxyl groups and the osmotic pressure exerted by mobile ions. As a result, an optically transparent microgel system with high elasticity was formed. The dense gels were subsequently thinned to the appropriate concentration by further blending with the NHs.

Rheological studies revealed that both BM entrapment and NHs incorporation had negligible influence on the rheological behavior of the gel formulations, all the Carbopol-based gels exhibited very similar rheological profiles. The plot of viscosity versus shear rate **(**Fig. 3**C)** demonstrated that the inclusion of BM-NHs into the formulation did not alter the shear-thinning behavior of the gel system. The viscosity of all samples decreased as the shear rate increased, a desirable property for topical applications, enabling easy dispensing from its container and uniform application onto the skin (Islam et al., 2004). The amplitude sweep test, depicted in Fig. 3**B**, illustrated the linear viscoelastic behavior of the gels. At lower strains, the elastic modulus (G') exceeded the viscous modulus (G"), indicative of a consistent tridimensional network structure akin to gel-like behavior in the systems. These formulations displayed a non-flowing nature unless exposed to high strains, withstanding structural deformation until a critical strain of approximately 50 %. The frequency sweep test **(**Fig. 3**D)** demonstrated no obvious change in storage modulus (G′) values across the tested frequency range of 0.1 to 10.0 Hz, suggesting substantial stability due to its robust crosslinking structure. The NHs incorporated gel formulation

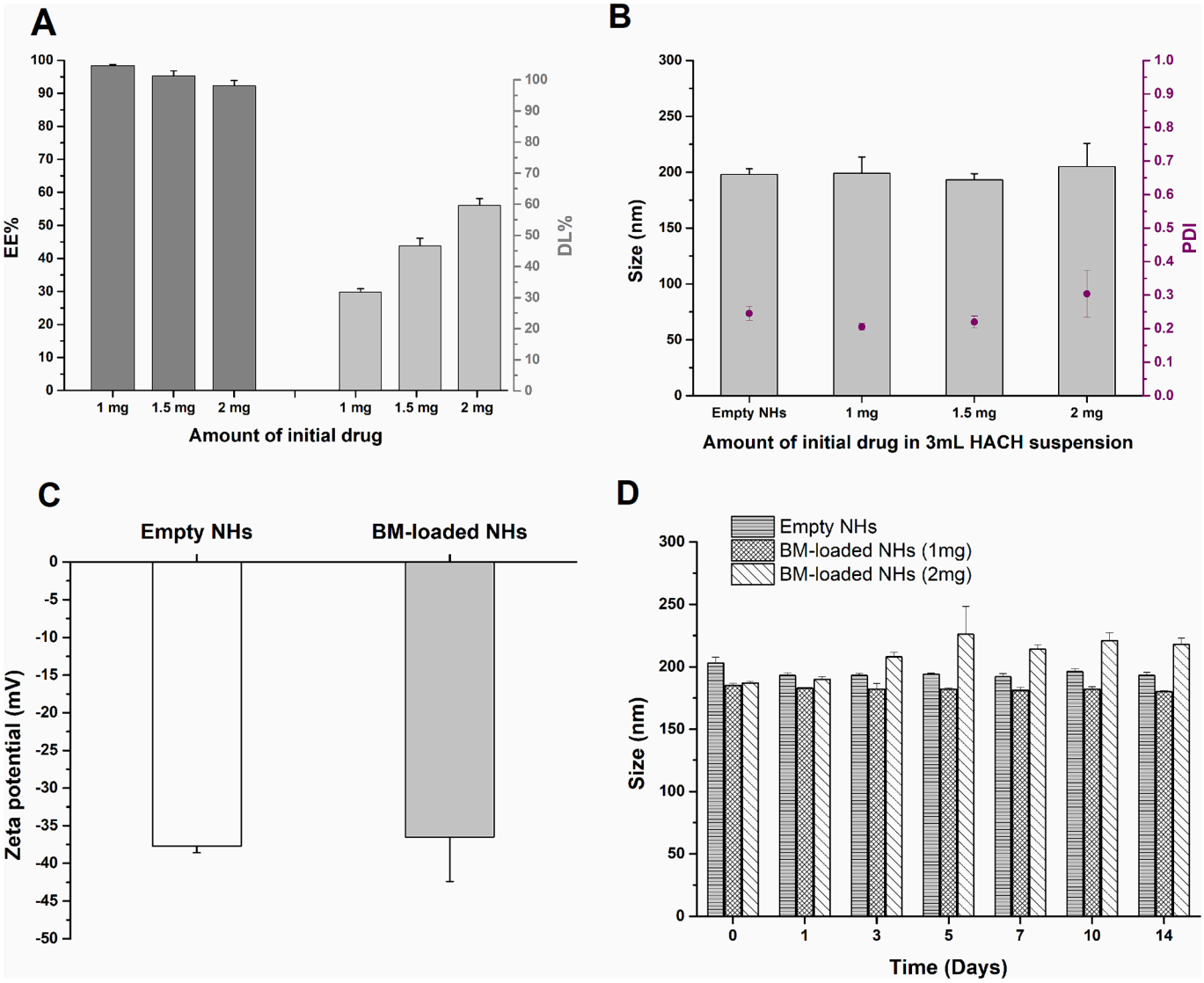

Fig. 1. Characterization of empty NHs and BM-loaded NHs. (A) EE% (dark bars) and DL% (light bars) of BM-loaded NHs at different drug concentrations, (B) mean diameter and PDI of empty and BM-loaded NHs with different drug amounts, (C) zeta-potential of empty and BM-loaded NHs, and (D) mean diameter of NHs as a function of time for stability at 4 ℃. All data are presented as mean value ± standard deviation. Each measurement was performed in triplicate (n = 3).

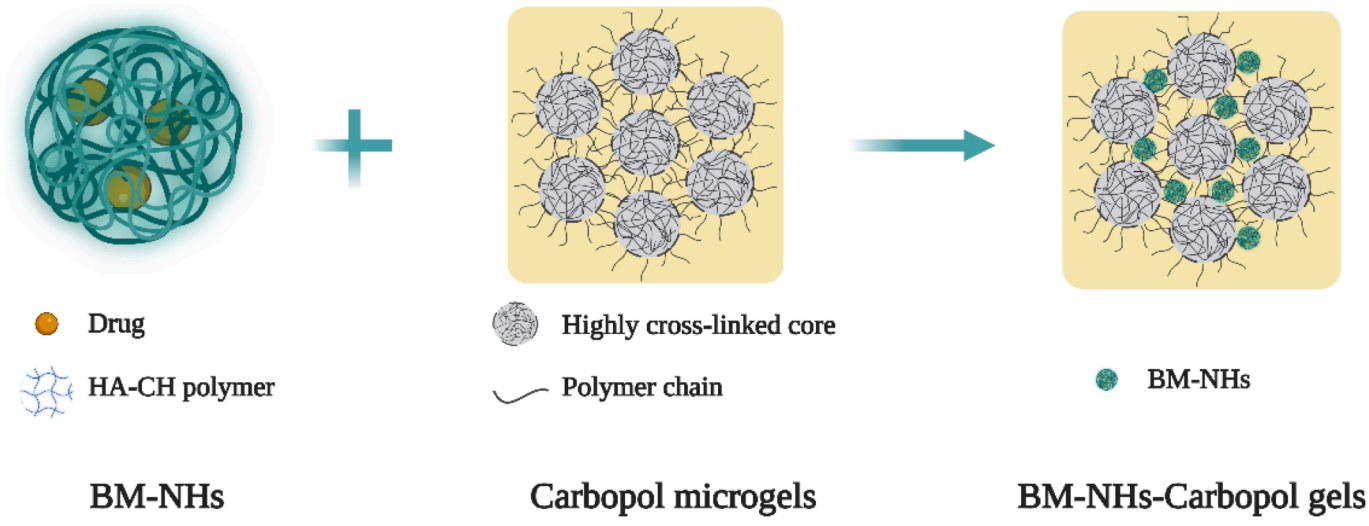

Fig. 2. A schematic illustration of the preparation process of BM-NHs-Carbopol gel formulation.

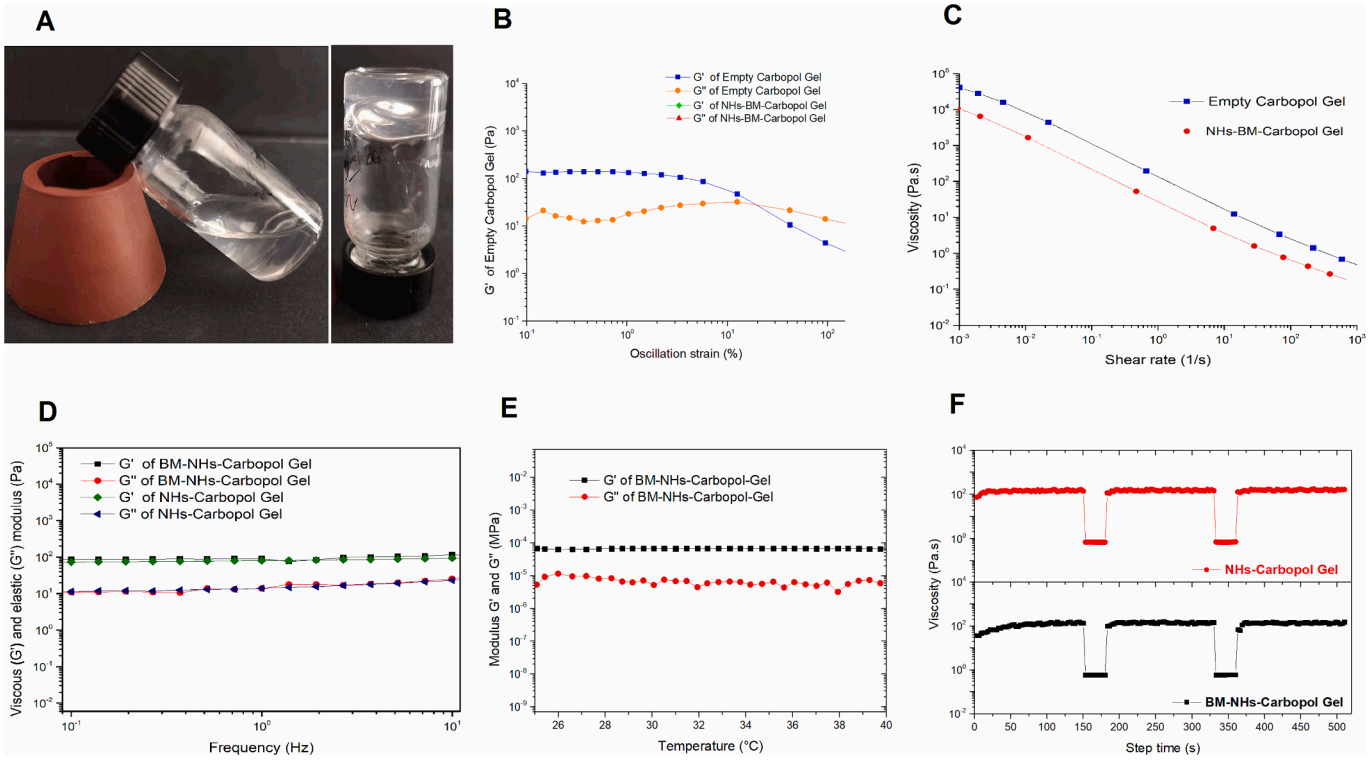

Fig. 3. Rheological characterizations of the gel systems. (A) Representative photographs of HACH NHs before and after incorporation with Carbopol, and the formation of BM-NHs-Carbopol gel (vertical vial). (B) Amplitude sweep test, (C) flow sweep curves: viscosity as a function of shear rate, (D) frequency sweep studies for empty NHs-Carbopol gel and BM-NHs-Carbopol gel. (E) Evaluation of the stability of gel formulation at a temperature range from 25 ℃ to 40 ℃, and (F) time-dependent flow behavior at shear cycles (recovery test) for NHs-Carbopol gel and BM-NHs-Carbopol gel.

exhibited significantly higher storage modulus (G′) in contrast to the loss modulus (G″), implying typical gel-like properties and good structural stability (Ying and Misran, 2017).

Moreover, a temperature sweep test was conducted to evaluate the rheological stability of the gel formulation **(**Fig. 3**E).** No discernible changes in complex modulus and viscosity were observed within a temperature range from 25 to 40 ℃ for both the NHs-Carbopol gel and BM-NHs-Carbopol gel. This indicates that the formulation does not undergo any phase transition and retains its intrinsic viscoelastic properties at both room temperature and normal body temperature. As depicted in Fig. 3**F**, the viscosity exhibited a rapid decline under the application of high shear rates, yet the gel's structure swiftly recovered over a defined period, even after undergoing five cycles of alternating low-shear and high-shear conditions. This characteristic is advantageous for topical application, ensuring ease of squeezing from a container, successful adherence to the skin, and effective spreading during application.

3.3. Evaluation of occlusive properties of Carbopol-Based gels and NHs

The percentage of water loss exclusively depends on the ability of the formulation to form an occlusive layer on the skin surface. The results of the occlusive test are represented in **Fig. S2**. Notably, there was a significant reduction in the percentage of water loss through the filter paper after 24 and 48 h for the BM-NHs-Carbopol gels compared to that of BM-NHs ($p < 0.001$). This decrease can be attributed to the enhanced occlusive property due to the formation of a thin film layer on the filter paper surface, as observed in the Carbopol-based gel formulation (Kakkar et al., 2018). The skin occlusive effect offered by the NHs-Carbopol gel could maintain hydration and alleviate symptoms such as itching, dryness and scaling, which are common clinical manifestations of dermatologic diseases. Furthermore, the high occlusive property, by decreasing *trans*-epidermal water loss, would improve the permeation ability of the formulation (Rapalli et al., 2021).

3.4. In vitro drug release studies

In vitro release studies were conducted to evaluate the drug release pattern from the formulations under standardized *in vitro* conditions. As shown in Fig. 4, the cumulative percentage of drug release was studied for BM-NHs, BM-NHs-Carbopol gel and a commercial solution (Ecoval®) as a control at both pH 5.5 and 7.4. For the commercial betamethasone valerate-based cutaneous solution, the results showed a rapid release of approximately 90 % of the drug within the initial 4 h, increasing to nearly 100 % after 8 h. In contrast, both the BM-NHs and BM-NHs-Carbopol gel exhibited a sustained drug release profile over 28 h, with the BM-NHs-Carbopol gel demonstrating a comparatively extended release duration. This release pattern was characterized by an initial rapid release phase followed by a slower and prolonged release, unlike the commercial solution. These findings suggest that the BM-NHs formulations can provide sustained release of the drug over an extended period compared to the rapid release observed with the commercial solution. The release of BM from the nanogel systems was more pronounced at pH 5.5 compared to pH 7.4, indicating that the HA-CH-based drug-loaded system exhibited greater release under acidic conditions. This characteristic is particularly advantageous for psoriasis treatment, given that psoriasis is associated with an inflammatory process that creates an acidic microenvironment (Gao et al., 2023).

The release mechanism of the loaded drug was governed by the swelling and degradation process of the NHs network upon solvent entry, followed by simple diffusion of the drug from NHs dispersed in the Carbopol matrix into the receptor medium. The kinetic data analysis indicated that the release pattern of BM from the NHs-Carbopol gel system followed a first-order release model with Tlag and Fmax parameters. The model exhibited the best fit with the highest R^2 values of 0.991 and 0.993 at pH 5.5 and 7.4, respectively. Further analysis using

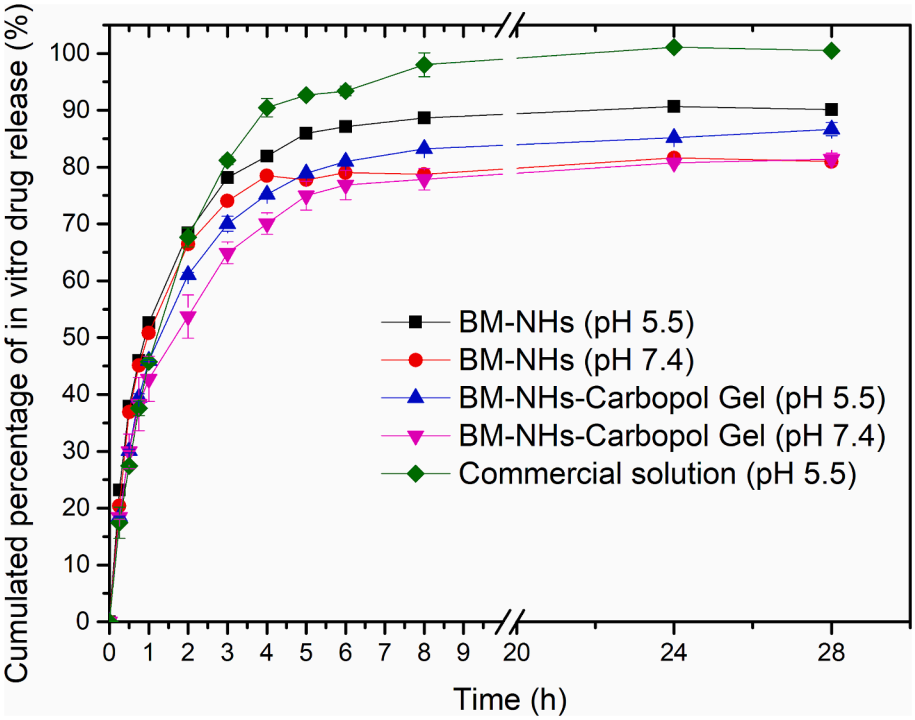

Fig. 4. *In-vitro* drug release profile of BM- NHs, BM-NHs-Carbopol gel and commercial solution (Ecoval®) at pH 5.5 and 7.4. Each experiment was conducted at least in triplicate.

the Korsmeyer-Peppas model suggested Fickian-type diffusion as the release exponent (n) value was less than 0.45 (Dash et al., 2010). These results are summarized in Table 1. Such a drug release profile of the NHs-Carbopol gel system appears to be advantageous for psoriasis treatment, as the initial rapid release phase could provide an adequate therapeutic dose, while the subsequent slow and sustained release can prevent rapid drug exposure to exfoliated psoriatic skin, thereby reducing systemic toxicity.

3.5. Permeability studies

3.5.1. In vitro Strat-M® membrane permeation

The cumulative drug retention, percentage of drug permeation and the permeation parameters into the Strat-M® membrane at each time point for all the formulations are presented in Fig. 5 and Table 2, respectively. For the NHs and NHs-Carbopol gel formulations, the initial amount of BM in the donor compartment of the Franz cell was measured to be 467 ± 23 µg and 415 ± 13 µg, respectively. As shown in Fig. 5**A and 5B**, the permeation of BM into the Strat-M® membrane exhibited a time-dependent pattern for both NHs and NHs-Carbopol gel formulations. Notably, the NHs formulation demonstrated a higher rate and greater amount of BM permeation at all observed time points compared to the NHs-Carbopol gel system. Specifically, the percentage of BM retention within the membrane, relative to the initial amount in the donor chamber, was found to be 10.1 ± 0.6 % and 4.4 ± 0.2 % for NHs and NHs-Carbopol gel after 2 h, respectively. This difference could be attributed to the higher viscosity of the NHs-Carbopol gel, which may lead to slower permeation and release of the drug. After 24 h of permeation, 29.7 ± 3.4 % and 19.0 ± 3.9 % of the initial amount of BM were extracted from the membrane for NHs and NHs-Carbopol gel, respectively. This suggests that the NHs formulation has a higher permeability rate compared to the NHs-Carbopol gel formulation.

Table 1
Kinetics models for drug release from NHs and NHs-Carbopol gel.

Type of formulation	First-order with Fmax (R^2)	First-order with Tlag and Fmax (R^2)	Korsmeyer-Peppas with F0		Korsmeyer-Peppas with Tlag	Hixson-Crowell with Tlag
			R^2	n		
BM loaded NHs (pH 5.5)	0.987	0.990	0.875	0.152	0.933	0.732
BM loaded NHs (pH 7.4)	0.978	0.985	0.887	0.183	0.932	0.755
BM loaded NHs/ Carbopol Gels (pH 5.5)	0.988	0.991	0.876	0.174	0.932	0.774
BM loaded NHs/ Carbopol Gels (pH 7.4)	0.992	0.993	0.844	0.123	0.924	0.567

During the initial 6 h of the permeation study, neither the NHs nor the NHs-Carbopol gels exhibited effective permeation across the membrane, making it difficult to quantify the amount of drug present in the receptor compartment. The data in Table 2 further illustrates this observation, showing that the majority of the permeated drug was retained within the membrane itself, while only negligible amounts of the drug permeated through to the receptor compartment. Besides, Fig. 5**D** shows the reduction in drug amount within the donor compartment, which corresponds closely to the amount of drug retained inside the membrane (as shown in Fig. 5**A**). These results demonstrated the minimal ability of BM to cross the membrane. The observed disparity in permeation rates between the NHs and NHs-Carbopol gel systems could be attributed to the slower release kinetics and higher viscosity associated with the Carbopol-based gels.

3.5.2. Ex vivo skin permeation and drug retention studies

The *ex vivo* skin permeation and drug deposition studies were

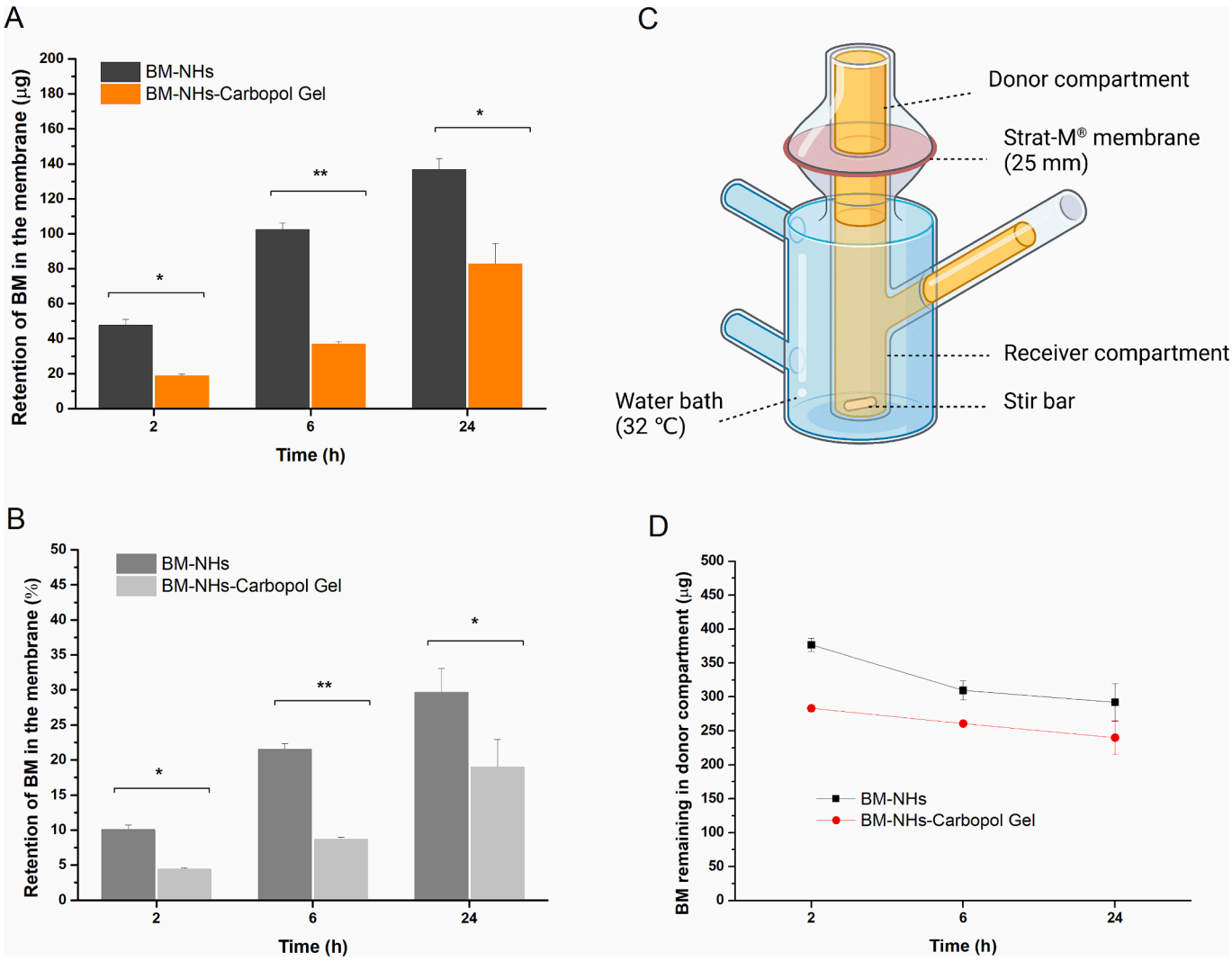

Fig. 5. *In-vitro* permeation studies. (A) The amount and (B) percent of BM permeated into Strat-M® membrane from the NHs and NHs-Carbopol gel at the end of each time point. (C) Experimental set-up of the Frans-cell (created with BioRender.com). (D) The amount of BM remaining in the donor compartment at the end of each time point. All data are presented as mean value ± standard deviation. Results were obtained in triplicate (n = 3), * $p < 0.05$, ** $p < 0.01$.

Table 2
In vitro permeation parameters for the NHs and NHs-Carbopol gel. Each data represents the mean ± standard deviation (n = 3).

Time (h)	Sample	Penetrated drug (μg)	J_{SS} (μg/cm^2/h)	$K_P \times 10^3$	Retained drug (μg)	J_{RR} (μg/cm^2/h)	$K_R \times 10^3$
6	BM-NHs	1.11 ± 0.12	0.29 ± 0.04	0.63 ± 0.12	102.4 ± 3.7	26.84 ± 0.96	58.35 ± 6.06
	BM-NHs-Carbopol gel	0.72 ± 0.08	0.19 ± 0.02	0.46 ± 0.04	37.1 ± 1.2	9.72 ± 0.30	23.77 ± 1.47
24	BM-NHs	5.97 ± 4.78	0.39 ± 0.31	0.83 ± 0.62	136.8 ± 6.3	8.96 ± 0.41	19.49 ± 2.22
	BM-NHs-Carbopol gel	3.72 ± 0.78	0.24 ± 0.05	0.60 ± 0.14	83.0 ± 11.5	5.44 ± 0.76	13.27 ± 1.44

conducted using excised porcine ear skin mounted on Franz diffusion cells for both BM-NHs and BM-NHs-Carbopol gels. Aliquots collected from the receptor compartment and the accumulated drug extracted from different skin layers were analyzed using HPLC. As shown in Fig. 6**A**, the results are expressed as a percentage of the initial amount of BM applied on the skin surface. The cumulative drug amount that permeated through the skin after 24 h was 26.9 ± 8.5 % for BM-NHs and 11.6 ± 1.8 % for BM-NHs-Carbopol gels (n = 3). The higher viscosity of Carbopol gels acts as a barrier, impeding the free permeation of the drug through the skin layers. This resulted in divergent permeation rates between NHs and Carbopol-based gel formulations. For the commercial Ecoval solution, the amount of detectable drug was negligible for the initial 4 h. Comparatively, the permeation flux of BM-NHs (5.33 ± 1.45 μg/cm^2/h) and BM-NHs-Carbopol gel formulation (3.08 ± 0.41 μg/cm^2/h) after 24 h was approximately 8.0-fold and 4.5-fold higher, respectively, than that of the commercial Ecoval solution (0.67 ± 0.18 μg/cm^2/h). The enhancement in permeation for both BM-NHs and BM-NHs-Carbopol gel formulations was expected due to the nanoscale size of the NHs system, leading to significantly improved drug delivery through the skin ($p < 0.001$).

The drug content retained in the skin was determined by extracting the drug from different layers of skin tissue after the 24-hour permeation experiments. The results revealed that the retained drug in the skin amounted to 3.79 ± 1.14 μg/h/cm^2, 2.74 ± 0.46 μg/h/cm^2 and 3.02 ± 1.16 μg/h/cm^2 for BM-NHs, BM-NHs-Carbopol gel and Ecoval solution (betamethasone valerate), respectively. The average percentage of the drug retained in the full layer of skin, relative to the initial drug amount in the donor compartment, was calculated to be 16.86 ± 5.96 %, 11.00

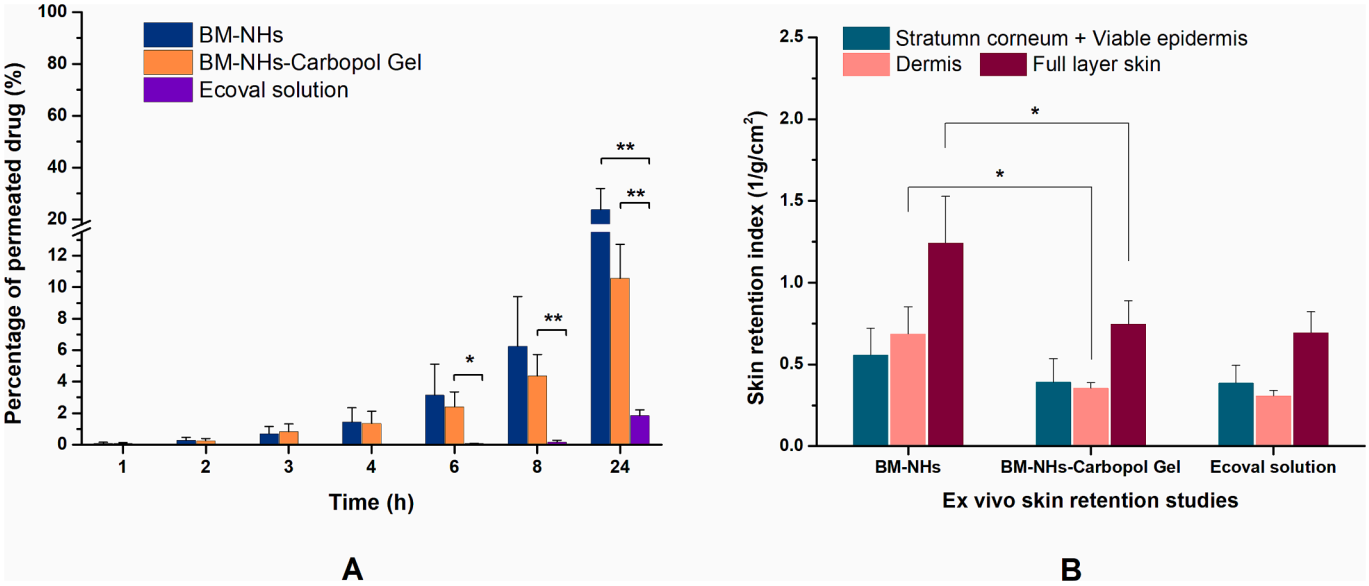

Fig. 6. *Ex-vivo* transdermal permeation profiles of BM-NHs, BM-NHs-Carbopol gel and Ecoval solution. (A) Comparison of permeated drug through the skin in different drug-loading systems. (B) Comparison of skin retention profiles of drug in different layers of skin after 24 h of exposure, results are represented as the retention indexes. Asterisks denote statistically significant differences (*p < 0.05, **p < 0.01).

± 1.75 % and 11.68 ± 4.62 % for BM-NHs, BM-NHs-Carbopol gel and Ecoval solution, respectively. However, the amount of drug retained in the skin depends not only on the permeation behaviour of the formulation but also on the thickness of the skin, which can introduce variability that is more challenging to control compared to commercial synthetic membranes. To describe the retention results objectively, a retention index was calculated according to the following equation:

$$I_{R24} = \frac{Q_R}{W_s \times A \times Q_0}$$

where I_{R24} is the skin retention index after 24 h, Q_R is the amount of retained drug (μg), Q_0 is the amount of initial drug (μg), W_s is the weight of the full layer of active skin available for permeation (g), and A is the active area available for permeation (0.64 cm^2).

As is shown in Fig. 6**B**, the skin retention index from BM-NHs (1.24 ± 0.29 $g^{-1}cm^{-2}$) is higher compared to other formulation systems. However, the index from BM-NHs-Carbopol gel (0.75 ± 0.14 $g^{-1}cm^{-2}$) is similar to that of the commercial solution (0.69 ± 0.13 $g^{-1}cm^{-2}$), even though the commercial solution contains an organic permeation enhancer (isopropyl alcohol). For all formulations, the drug effectively retained in both the epidermis and dermis layers. For BM-NHs-Carbopol gel, the indexes are 0.39 ± 0.14 $g^{-1}cm^{-2}$ in the epidermis and 0.35 ± 0.04 $g^{-1}cm^{-2}$ in the dermis.

The skin retention results suggest that a similar amount of drug was retained in both the visible epidermis and dermis layers, despite the dermis being anatomically thicker than the epidermis. This highlights the advantage of NHs-based formulations for targeted delivery to the skin layers for effective psoriasis therapy, as these layers are mainly affected by psoriasis (Shah et al., 2012). Moreover, increased skin retention can help minimize systemic adverse effects related to the drug.

3.6. Evaluation of biological activity on HaCaT keratinocytes

Both empty and BM-loaded NHs (NHs-BM) cytotoxicity was assessed using the MTT assay on HaCaT cells. When exposed to various concentrations (ranging from 1 to 100 μg/mL) of polymer, NHs did not exhibit obvious cytotoxicity at certain concentrations. The results depict the percentage of cell viability after a 24-hours of treatment (**Fig. S3**).

We evaluated the modulation of the pro-inflammatory cytokines IL-33 and IL-25 in HaCaT cells stimulated with IFN-γ and then treated with BM or NHs-BM (Fig. 7**A**). Secretion (or expression) of IL-33 was significantly reduced with the addition of BM or NHs-BM, compared to the IFN-γ-stimulated control (IFN-γ + DMSO). On the other hand, IL-25 secretion (or expression) was not modified in HaCaT cells in the unstimulated and IFN-γ + DMSO samples. We also assessed the modulation of LORICRIN (LOR) and FILAGGRIN (FLG), two very important proteins involved in inflammation and modulation of skin barrier integrity, under the same conditions (Fig. 7**B**). Results show that NHs-BM significantly increased *LOR* expression compared to the IFN-γ-stimulated control. Additionally, *FLG* was reported to be down-modulated by both NHs and NHs-BM compared to the IFN-γ-stimulated control, bordering on statistical significance (p = 0.0509 and p = 0.0522, respectively).

To verify the applicability of these NHs-BM, we decided to study their anti-inflammatory effects on human skin equivalents, produced by the Mattek® company, treated or untreated with 200 ng/mL of INF-γ. We found that IL-25 (Fig. 8**A**) is downmodulated by NHs (borderline statistical significance, p = 0.08), and by NHs-BM, although not statistically significant, but to a greater extent than by treatment with BM alone. In the case of IL-33, although not statistically significant, a similar decrease was observed in the HaCaT experiment with the presence of BM and NHs-BM. Moreover, we detected a statistically significant reduction of IL-37 in the NHs-treated group (Fig. 8**B**).

Fig. 8**C** shows a positive trend of NHs and NHs-BM in the modulation of LOR and FLG compared to BM, although not statistically significant. In Fig. 8**D**, there is an increase in the expression of CD44s (not statistically significant) and CD44v6 (borderline significant, p = 0.07) in NHs-BM-treated compared to BM. Finally, we assessed *TNF-α* expression (Fig. 8**E**), showing that the IFNγ + NHs group is statistically significant compared to the other inflamed groups (p < 0.05).

4. Discussion

Topical treatment is an advantageous administration route for achieving direct dermal delivery of therapeutics to disease sites in inflammation-associated skin diseases, including atopic dermatitis and psoriasis (Jebbawi et al., 2020a). Delivering anti-inflammatory drugs directly to the inflamed sites can provide targeted treatment with potentially fewer systemic side effects. However, the stratum corneum

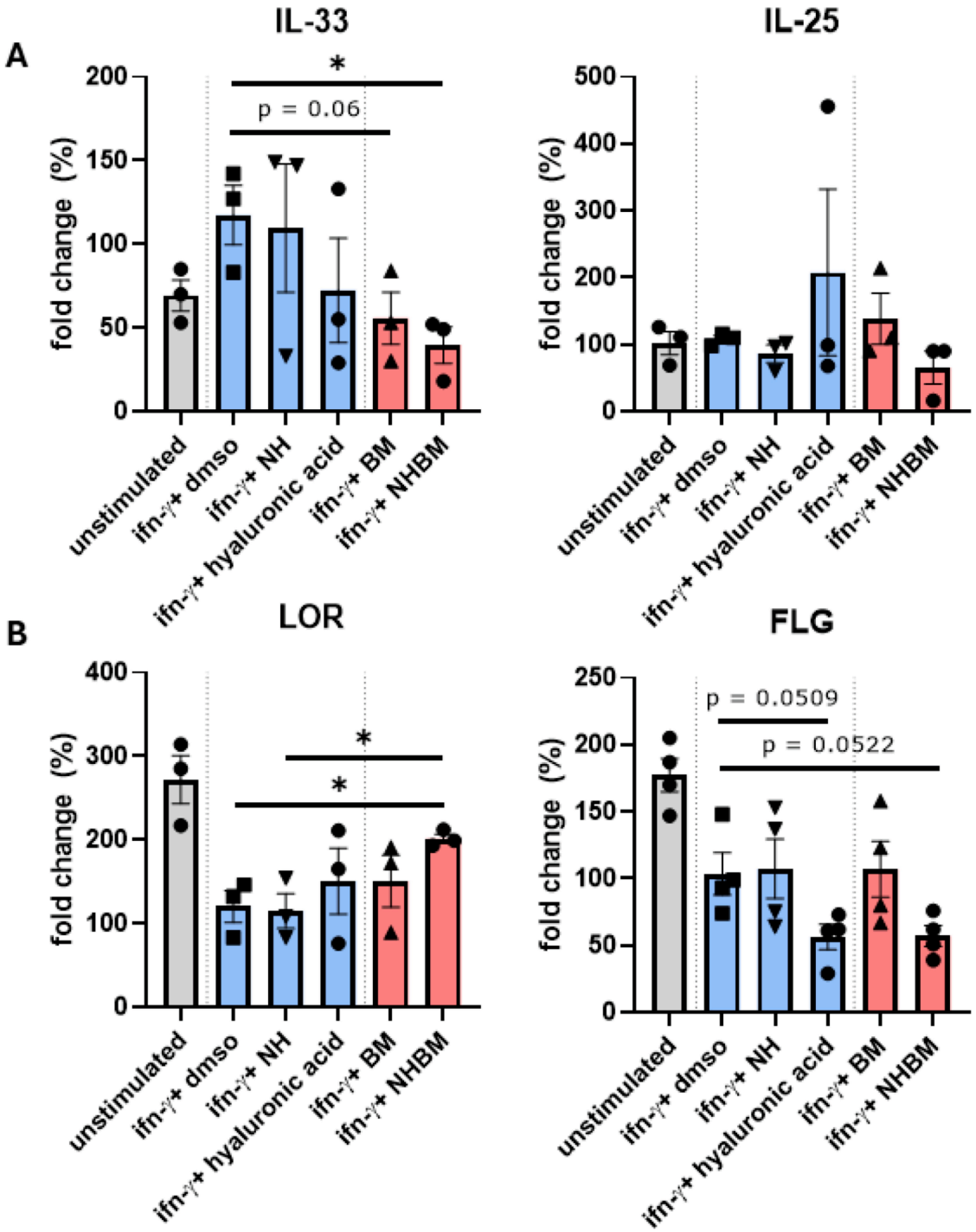

Fig. 7. Modulation of cytokines and skin integrity proteins in HaCaT Cells. Percentage expression of (A) proinflammatory cytokines IL-33 and IL-25, (B) protein involved in skin integrity *LORICRIN* (*LOR*) and *FILAGGRIN* (*FLG*) on HaCaT cell line following 24-hour exposure to DMSO, BM, NHs, high molecular weight hyaluronic acid or NHs-BM in pro-inflammatory condition (IFN-γ-stimulated cells). All data are presented as mean value ± SEM. Results were obtained in biological triplicate (n = 3), * $p < 0.05$ according to Welch's ANOVA test.

acts as a formidable obstacle for drug molecules, making it difficult for them to pass through and reach deeper skin layers effectively. This poses a significant challenge in topical dermal therapy, particularly in cases where the epidermis is thickened due to conditions like psoriasis.

HA-CH-based NHs offer a promising tool in drug delivery for several compelling reasons. As a biocompatible and biodegradable polysaccharide, HA has been already extensively recognized and utilized in the field of drug delivery (Zhang et al., 2019). Cholesterol, a vital component of cell membranes, is widely distributed in the human body, and its derivatives have been widely developed as carriers in drug delivery systems (Ruwizhi and Aderibigbe, 2020). Previous works have demonstrated that HA-CH-based formulations can enhance ocular drug delivery by prolonging retention time in the preocular area and facilitating drug permeation (Zoratto et al., 2021a).

To prepare an amphiphilic polymer carrier of HA-CH, the carboxyl groups of HA were linked to cholesterol moieties through covalent bonds. This conjugation allowed the resulting compound to self-assemble into nanoscale NHs under specific conditions. Notably, the

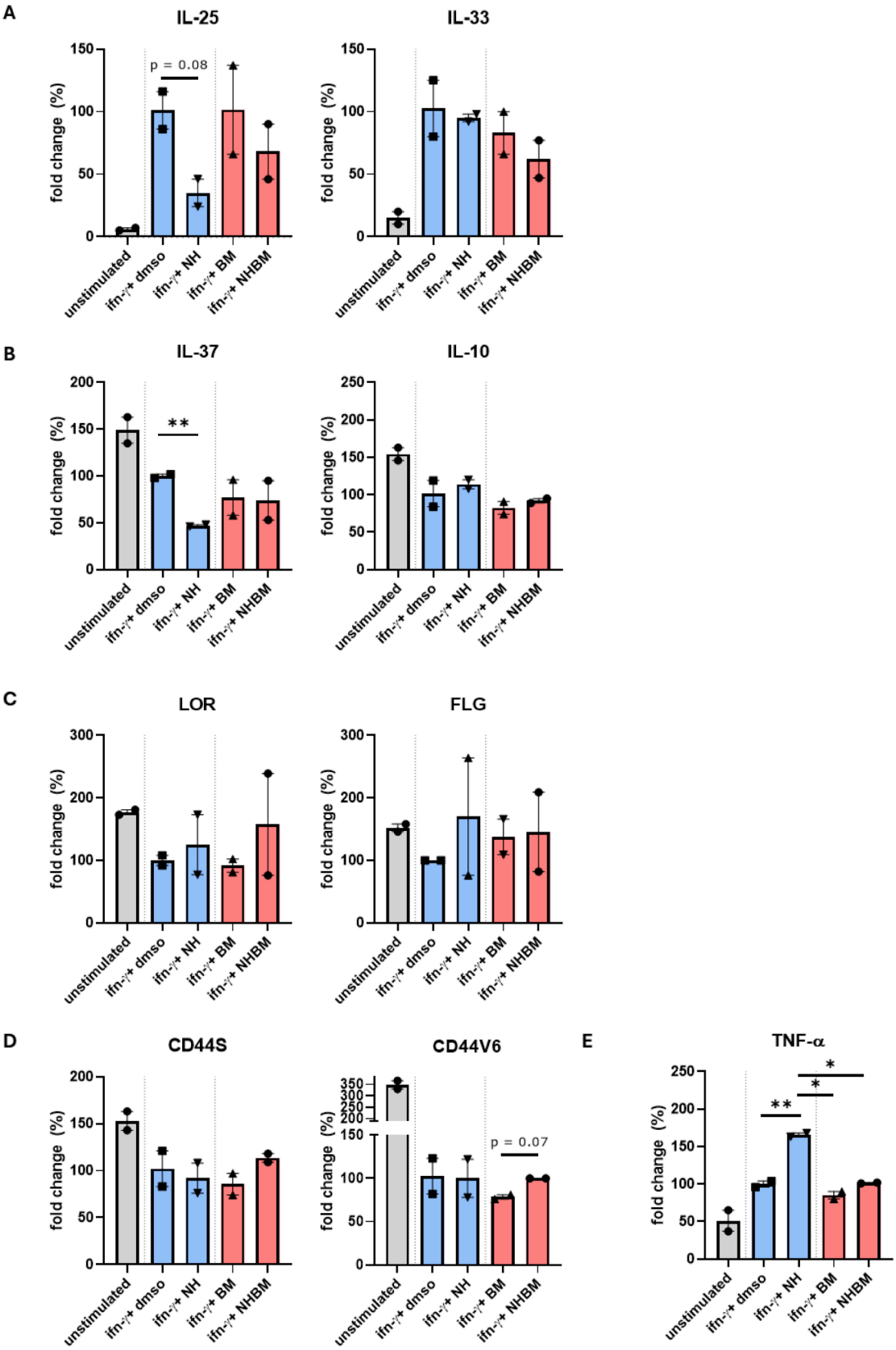

Fig. 8. Modulation of cytokines and proteins in EpiDermFT™ model. Percentage expression of (A) proinflammatory cytokines IL-25, IL-33, (B) anti-inflammatory cytokines IL-37, IL-10, (C) protein involved in skin integrity LOR and FLG, (D) standard (CD44s) and alternative (CD44V6) splicing variant for hyaluronic acid receptor, (E) TNF-α on EpiDermFT™ following 24-hour exposure to DMSO, BM solution, NHs or BM-loaded NHs in pro-inflammatory condition (IFN-γ-stimulated cells). All data are presented as mean value ± SEM. Results were obtained in biological duplicate (n = 2), * $p < 0.05$ according to Welch's ANOVA test.

innovative application of autoclave treatment (121 ℃, 1.1 bar, 20 min) during NHs preparation allows for the production of sterile products in a single step with high drug-loading efficiency and reproducibility. This is particularly appealing for large-scale applications, although this method may not be suitable for thermo-sensitive drugs, such as betamethasone valerate (Zoratto et al., 2021b). In this study, the successful loading of BM into NHs was achieved with an impressive encapsulation efficiency (EE%) of up to 98 % (Fig. 1**A**), which is higher than that of dexamethasone (a structural isomer of BM) reported in previous work (Zoratto et al., 2021a). The excellent drug-loading capability can be attributed to the hydrophobic interactions between the drug molecules and the hydrophobic regions present in the polymer chains, facilitated by the incorporation of cholesterol moieties. The higher EE% achieved for BM loaded in HA-CH can be attributed to its stronger hydrophobicity (LogP 1.94) compared to that of dexamethasone (LogP 1.83), resulting in stronger hydrophobic interactions with polymer chains. The improved apparent water solubility of the active pharmaceutical ingredient (API) can enhance the bioavailability of the drug. Besides, the prepared BM-NHs formulation exhibited favorable size distribution, PDI, and zeta-potential for potential biomedical applications. Furthermore, the formulation demonstrated excellent stability under both refrigerated and long-term storage conditions. Based on the above-mentioned properties and the characterization of BM-loaded HA-CH NHs, HA-CH can be considered a promising carrier candidate for loading BM, especially beneficial for the treatment of skin diseases. It's worth noting that HA-CH has proven effective for encapsulating both hydrophobic and hydrophilic drugs, making it versatile for various pharmaceutical applications.

Development of NHs-Carbopol gel formulation for topical applications

For the development of an effective topical formulation suitable for cutaneous applications, Carbopol was selected as the gelling agent for preparing the NHs-Carbopol gel formulation. This selection was due to its biocompatibility, distinctive swelling, and subsequent rheological behavior after neutralization. The Carbopol family of polymers has been approved by the FDA and is widely used in commercial drug delivery systems (Graziano et al., 2021). Moreover, it has garnered growing interest in research for developing innovative formulations in skin drug delivery (Calderon-Jacinto et al., 2022; Pandey et al., 2020; Zheng et al., 2016). The rheological response of Carbopol solutions primarily depends on concentration and pH. In a study employing the method of multiple-particle tracking, Oppong et al. have demonstrated that Carbopol gel comprises two coexisting regions, including elastic regions formed by highly crosslinked microgel cores and surrounding shell of viscous regions containing polymer chains (Oppong et al., 2006). At low Carbopol concentrations, the tracer particles can move freely within the viscous region environment. However, as the polymer concentration increases, the interpenetration of microgel particles leads to the formation of elastic regions with higher entanglement or crosslink density, resulting in a decrease in the proportion of the viscous environment. Kowalczyk et al. (Kowalczyk et al., 2015) also reported that as the polymer concentration increases from 0.1 % to 0.75 % the weight fraction of particles in the viscous environment decreases from 85 % to 15 %. In our study, the final concentration of Carbopol in the gel formulation is 0.25 %, which does not restrict the movement of BM-NHs particles (~200 nm). It is hypothesized that the BM-NHs particles, much smaller in size than the mesh size of the polymer network, can move freely within the Carbopol gel. Angle light scattering experiments conducted by Lee et. al. demonstrated that Carbopol gel solutions consist of crosslinked cores with a diameter of approximately 500 nm, surrounded by an expanded shell of polymer chines measuring around 20 μm in size (Lee et al., 2011).

All the rheological and permeation results can be explained by the interactions between BM-NHs and the microstructure of Carbopol gel discussed above. The gel formulations we prepared were transparent and homogeneous, and there were no obvious changes in rheological properties after the entrapment of the drug in the system. Moreover, the same *in vitro* drug release model was fitted for BM in both the NHs and NHs-Carbopol based systems, indicating that the drug was released in a controlled manner by a combination of erosion and diffusion mechanisms. The incorporation of Carbopol contributes to the slower and sustained drug release, likely due to the increased viscosity of the gel formulation, which in turn elongates the diffusion pathway compared to NHs alone.

In vitro and *ex vivo* permeation

The *in vitro* permeation behaviors of NHs and NHs-Carbopol systems were evaluated using synthetic Strat-M® membranes. Due to its multi-layer composition, this synthetic membrane is considered a viable model for mimicking the intact skin barrier. The use of Strat-M® membranes was endorsed in 2018 in the guideline drafted by the European Medicines Agency as a suitable approach to better comprehend and characterize the performance of topical and transdermal formulations (Bolla et al., 2020). Additionally, these synthetic membranes are cost-effective, readily available, and exhibit excellent data reproducibility (Zsikó et al., 2019). Several previously published studies have demonstrated that Strat-M® membrane, with less variability and storage limitations, had a good interrelationship with human skin to measure the permeability potentiality of both hydrophilic and lipophilic therapeutic compounds (Bolla et al., 2020; Haq et al., 2018a; Kaur et al., 2018). Given these advantages, Strat-M® membranes were employed in this study to investigate the permeability characteristics of NHs-based formulations.

Although the synthetic artificial membrane (Strat-M®) offers several advantages for transdermal delivery research compared to the biological skin, it may not fully reflect the actual drug permeation but rather focuses solely on drug release. Moreover, it cannot provide comprehensive insight into the interaction between formulation components and the skin (Neupane et al., 2020). Among many permeation studies involving Strat-M® membrane, some reported consistent permeation parameters between the synthetic membrane and actual skin (Haq et al., 2018b; Kovács et al., 2021). However, there have also been instances where differing permeation results were observed (de Almeida Borges et al., 2013). In this work, inconsistent permeation behaviours were observed between the Strat-M® membrane and pig ear skin for our prepared formulations. More specifically, the drug fluxes (J_{SS}) and permeability coefficients (K_P) of BM from the Strat-M® are found to be negligible, contrasting with the obvious drug permeation observed through actual skin after 24 h under the same conditions. In skin permeation, the foremost barrier is the outermost stratum corneum layer, whereas the rate-limiting layer for synthetic artificial membranes remains less defined (Neupane et al., 2020). Notably, both BM-NHs and BM-NHs-Carbopol gel formulations were retained within the Strat-M® membrane even after a 2-hours permeation period, although the dissection of distinct membrane layers remains a challenge. We also conducted the permeation experiments for a commercial solution using the Strat-M® membrane (data not shown), nevertheless, the integrity of the membrane was susceptible due to the presence of isopropyl alcohol in the commercial formulation. Despite the inclusion of an organic component as a permeation enhancer, the skin permeation and retention capabilities of the commercial solution were lower compared to the nano-delivery systems. Surprisingly, the commercial solution exhibited minimal skin permeation after 24 h (less than 2 %).

The nanoscale size of the NHs-based formulations enhances drug permeation across the stratum corneum, while the higher lipophilicity of the polymer carrier promotes retention in the lipophilic membrane of the skin, leading to greater drug deposition compared to the commercial solution. Moreover, the superior skin (instead of Strat-M® membrane) permeation and excellent skin retention properties of HA-CH NHs-based formulations can be attributed to several factors. In addition to the

smaller particle size, the cholesterol moieties within the polymer increase lipophilicity, while interactions between HA moieties and CD44 receptors on skin cells further enhance the permeation process. It is also important to consider the potential impact of prolonged NHs exposure (e.g., 24 h) on skin integrity, as extended exposure may lead to overhydration.

Evaluation of inflammatory parameters and tissue integrity on HaCaT cells and EpiDermFT™ model

Some pro-inflammatory cytokines, such as IL-33 and IL-25, are emerging as important cytokines involved in various inflammatory skin diseases, such as atopic dermatitis and psoriasis (Duan et al., 2019; Tsuji et al., 2023; Xu et al., 2018; Zeng et al., 2021). Specifically, these cytokines are produced by keratinocytes following damage or in response to other cytokines produced by immune system cells, such as IL-17.

NHs-BM showed a very good effect on IL-33, similar to BM, but not on IL-25 on HaCaT cell line. This result could be explained by the fact that in isolated keratinocytes, the inflammatory stimulus was not sufficient to induce the expression of this cytokine, which instead occurs in a model that also contains fibroblasts (i.e. EpiDermFT).

Considering tissue integrity, LOR is positively modulated in a statistically significant manner by NHs-BM. In line with our data, Wang (Wang et al., 2024) demonstrated that various hyaluronic acid-based hydrogels can stimulate LOR expression. The down-modulation of FLG, on the other hand, stimulated by NHs and NHs-BM, aligns with the effect observed by Huth (Marquardt et al., 2020) on a skin model 5 days after the administration of different fillers containing hyaluronic acid. Contrary to this evidence, human keratinocytes CHK administered with large molecular weight HA resulted in an almost 2.5-fold increase in filaggrin (Bourguignon, 2014). This finding, although contradicting our data on HaCaT cells, aligns with the data obtained on the EpiDermFT model, where a trend towards an increase in FLG and LOR after treatment with NHs and NHs-BM is evident. Probably this divergence occurs because HaCaT cells are immortalised human cells, whereas the CHKs and normal human epidermal keratinocytes (NHEK) present in the EpiDermFT are primary cells.

In the EpiDermFT model, we also showed that NHs-BM has a similar effect to BM regarding its impact on the pro-inflammatory cytokines IL-25 and IL-33, as well as on the anti-inflammatory cytokines IL-37 and IL-10. Interestingly, we have shown that empty NHs have an intrinsic anti-inflammatory effect *per se*, consistent with what is known in the literature on hyaluronic acid (Chen et al., 2018).

Concerning the down-modulation of IL-37 by NHs, to our knowledge, this phenomenon has not been described before, and there seems to be an interesting similar trend between the pro-inflammatory cytokine IL-25 and the anti-inflammatory IL-37. Further studies will be conducted in this area.

Finally, we evaluated the expression of the hyaluronic acid receptor CD44. It is known in the literature that corticosteroids (such as BM) can inhibit fibroblasts' proliferation and synthesis of extracellular matrix, including hyaluronic acid (Barnes et al., 2015), which impacts the expression of CD44 (Kaya et al., 2006). Regarding CD44s, we found no major differences among treatments, whereas we recorded a statistically significant increase in CD44v6 of NHs-BM compared to BM. CD44V6 is an alternative splicing variant of the protein involved in many biological processes (Ma et al., 2019), which was studied to validate the analysis of CD44s. The increase of both splicing variants in the NHs-BM-treatment appears consistent in comparison with the BM-treatment and could be due to the obvious presence of hyaluronic acid in the hydrogel. One of the factors involved in skin remodelling is TNF-α, which appears to be positively modulated by NHs treatment. Already Barshishat (Barshishat et al., 2002) observed that TNF-α can modulate the expression of CD44 splicing variant 6, but not the standard variant of CD44 (CD44s). Mechanistically, it can be envisaged that NHs were able to activate TNF-α which in turn led to a modulation in the expression of CD44.

5. Conclusions

In summary, HA-CH-based NHs and NHs-Carbopol nano-systems were developed and evaluated for the topical delivery of BM in potential psoriasis therapy. Both *in vitro* (Strat-M® membrane model) and *ex-vivo* (pig ear skin model) studies demonstrated that this BM-loaded nanocarrier can effectively enhance skin permeation and promote retention in deeper skin layers, proving to be superior to the commercial formulation. The HA-CH NHs-based formulation emerges as a promising carrier due to its advantageous characteristics such as small size (~190 nm), high EE%, excellent stability, favorable rheological properties, surface occlusive effect, and sustained drug release profile. The effective stratum corneum permeation of BM-loaded nanocarrier and greater retention in the deeper layers of the epidermis and dermis makes it a valuable candidate for topical psoriasis therapy. Moreover, the NHs system showed promising anti-psoriatic activity in an *in vitro* human 2D and 3D skin tissue model by downregulating proinflammatory cytokines. However, further studies are required to assess the therapeutic effect of this carrier system in an *in vivo* psoriasis model and to confirm the specific interactions between the carrier and skin receptors at the molecular level.

CRediT authorship contribution statement

Ju Wang: Writing – review & editing, Writing – original draft, Validation, Methodology, Investigation, Formal analysis, Data curation, Conceptualization. **Daniel Di Risola:** Writing – review & editing, Writing – original draft, Validation, Methodology, Investigation, Data curation. **Roberto Mattioli:** Writing – review & editing, Validation, Methodology, Investigation, Data curation. **Nicole Zoratto:** Writing – review & editing, Validation, Methodology, Investigation, Data curation. **Luciana Mosca:** Writing – review & editing, Supervision, Resources, Conceptualization. **Chiara Di Meo:** Writing – review & editing, Supervision, Project administration. **Pietro Matricardi:** Writing – review & editing, Writing – original draft, Supervision, Project administration, Funding acquisition, Conceptualization.

Declaration of competing interest

The authors declare that they have no known competing financial interests or personal relationships that could have appeared to influence the work reported in this paper.

Acknowledgements

The authors thank Dr. Cristina M. Failla, PhD, Experimental Immunology Laboratory, IDI-IRCCS, Rome, Italy, for her invaluable contribution to the data discussion. This work was supported by "Ricerche Ateneo" grant RM12117A81AEF242 and grant RM12117A81AEF242. RM recipient of funding from FSE REACT-EU, within the program PON "Research and Innovation" 2014–2020 (PON R&I), Action IV.6 "Contratti di ricerca su tematiche Green".

Appendix A. Supplementary data

Supplementary data to this article can be found online at https://doi.org/10.1016/j.ijpharm.2024.124978.

Data availability

Data will be made available on request.

References

Armstrong, A.W., Bagel, J., Van Voorhees, A.S., Robertson, A.D., Yamauchi, P.S., 2015. Combining biologic therapies with other systemic treatments in psoriasis: evidence-

based, best-practice recommendations from the medical board of the national psoriasis foundation. JAMA Dermatol. 151, 432–438.
Ayala-Fontánez, N., Soler, D.C., McCormick, T.S., 2016. Current knowledge on psoriasis and autoimmune diseases. Psoriasis (Auckland, NZ) 6, 7.
Baboota, S., Alam, M.S., Sharma, S., Sahni, J.K., Kumar, A., Ali, J., 2011. Nanocarrier-based hydrogel of betamethasone dipropionate and salicylic acid for treatment of psoriasis. International Journal of Pharmaceutical Investigation 1, 139–147.
Barnes, L., Kaya, G., Rollason, V., 2015. Topical corticosteroid-induced skin atrophy: a comprehensive review. Drug Saf. 38, 493–509.
Barshishat, M., Ariel, A., Cahalon, L., Chowers, Y., Lider, O., Schwartz, B., 2002. TNFα and IL-8 regulate the expression and function of CD44 variant proteins in human colon carcinoma cells. Clin. Exp. Metastasis 19, 327–337.
Bartosova, L., Bajgar, J., 2012. Transdermal drug delivery in vitro using diffusion cells. Curr. Med. Chem. 19, 4671–4677.
Bayer, I.S., 2020. Hyaluronic acid and controlled release: a review. Molecules (Basel, Switzerland) 25.
Boer, D.E.C., Mirzaian, M., Ferraz, M.J., Nadaban, A., Schreuder, A., Hovnanian, A., van Smeden, J., Bouwstra, J.A., Aerts, J., 2020. Glucosylated cholesterol in skin: Synthetic role of extracellular glucocerebrosidase. Clinica Chimica Acta; International Journal of Clinical Chemistry 510, 707–710.
Bolla, P.K., Clark, B.A., Juluri, A., Cheruvu, H.S., Renukuntla, J., 2020. Evaluation of formulation parameters on permeation of ibuprofen from topical formulations using strat-M® membrane. Pharmaceutics 12, 151.
Bourguignon, L.Y., 2014. Matrix hyaluronan-activated CD44 signaling promotes keratinocyte activities and improves abnormal epidermal functions. Am. J. Pathol. 184, 1912–1919.
Calderon-Jacinto, R., Matricardi, P., Gueguen, V., Pavon-Djavid, G., Pauthe, E., Rodriguez-Ruiz, V., 2022. Dual nanostructured lipid carriers/hydrogel system for delivery of curcumin for topical skin applications. Biomolecules 12.
Chen, L.H., Xue, J.F., Zheng, Z.Y., Shuhaidi, M., Thu, H.E., Hussain, Z., 2018. Hyaluronic acid, an efficient biomacromolecule for treatment of inflammatory skin and joint diseases: A review of recent developments and critical appraisal of preclinical and clinical investigations. Int. J. Biol. Macromol. 116, 572–584.
Coda, A.B., Icen, M., Smith, J.R., Sinha, A.A., 2012. Global transcriptional analysis of psoriatic skin and blood confirms known disease-associated pathways and highlights novel genomic "hot spots" for differentially expressed genes. Genomics 100, 18–26.
Dash, S., Murthy, P.N., Nath, L., Chowdhury, P., 2010. Kinetic modeling on drug release from controlled drug delivery systems. Acta Pol Pharm 67, 217–223.
de Almeida Borges, V.R., Simon, A., Sena, A.R.C., Cabral, L.M., de Sousa, V.P., 2013. Nanoemulsion containing dapsone for topical administration: a study of in vitro release and epidermal permeation. Int. J. Nanomed. 8, 535.
Dhar, S., Seth, J., Parikh, D., 2014. Systemic side-effects of topical corticosteroids. Indian J. Dermatol. 59, 460.
Du, X., Zhou, J., Shi, J., Xu, B., 2015. Supramolecular hydrogelators and hydrogels: from soft matter to molecular biomaterials. Chem. Rev. 115, 13165–13307.
Duan, Y., Dong, Y., Hu, H., Wang, Q., Guo, S., Fu, D., Song, X., Kalvakolanu, D.V., Tian, Z., 2019. IL-33 contributes to disease severity in Psoriasis-like models of mouse. Cytokine 119, 159–167.
Fakhari, A., Berkland, C., 2013. Applications and emerging trends of hyaluronic acid in tissue engineering, as a dermal filler and in osteoarthritis treatment. Acta Biomater. 9, 7081–7092.
Filippone, A., Consoli, G.M.L., Granata, G., Casili, G., Lanza, M., Ardizzone, A., Cuzzocrea, S., Esposito, E., Paterniti, I., 2020. Topical delivery of curcumin by choline-calix[4]arene-based nanohydrogel improves its therapeutic effect on a psoriasis mouse model. Int J Mol Sci 21.
Gao, X., Zhang, F., Huang, Y., Hu, W., Chen, Y., Jiang, L., Pan, X., Wu, C., Lu, C., Peng, T., 2023. Site-specifically launched microneedles for the combined treatment of psoriasis-diabetic comorbidity. ACS Appl. Mater. Interfaces.
Graziano, R., Preziosi, V., Uva, D., Tomaiuolo, G., Mohebbi, B., Claussen, J., Guido, S., 2021. The microstructure of Carbopol in water under static and flow conditions and its effect on the yield stress. J. Colloid Interface Sci. 582, 1067–1074.
Haq, A., Dorrani, M., Goodyear, B., Joshi, V., Michniak-Kohn, B., 2018a. Membrane properties for permeability testing: Skin versus synthetic membranes. Int. J. Pharm. 539, 58–64.
Haq, A., Goodyear, B., Ameen, D., Joshi, V., Michniak-Kohn, B., 2018b. Strat-M® synthetic membrane: Permeability comparison to human cadaver skin. Int. J. Pharm. 547, 432–437.
Islam, M.T., Rodriguez-Hornedo, N., Ciotti, S., Ackermann, C., 2004. Rheological characterization of topical carbomer gels neutralized to different pH. Pharm. Res. 21, 1192–1199.
Jebbawi, R., Fruchon, S., Turrin, C.-O., Blanzat, M., Poupot, R., 2020a. Supramolecular and macromolecular matrix nanocarriers for drug delivery in inflammation-associated skin diseases. Pharmaceutics 12, 1224.
Jebbawi, R., Fruchon, S., Turrin, C.O., Blanzat, M., Poupot, R., 2020b. Supramolecular and macromolecular matrix nanocarriers for drug delivery in inflammation-associated skin diseases. Pharmaceutics 12.
Kakkar, V., Kaur, I.P., Kaur, A.P., Saini, K., Singh, K.K., 2018. Topical delivery of tetrahydrocurcumin lipid nanoparticles effectively inhibits skin inflammation: In vitro and in vivo study. Drug Dev. Ind. Pharm. 44, 1701–1712.
Kaur, A., Katiyar, S.S., Kushwah, V., Jain, S., 2017. Nanoemulsion loaded gel for topical co-delivery of clobitasol propionate and calcipotriol in psoriasis. Nanomedicine: Nanotechnology Biology and Medicine 13, 1473–1482.
Kaur, L., Singh, K., Paul, S., Singh, S., Singh, S., Jain, S.K., 2018. A mechanistic study to determine the structural similarities between artificial membrane strat-M™ and biological membranes and its application to carry out skin permeation study of amphotericin B nanoformulations. AAPS PharmSciTech 19, 1606–1624.
Kaya, G., Tran, C., Sorg, O., Hotz, R., Grand, D., Carraux, P., Didierjean, L., Stamenkovic, I., Saurat, J.-H., 2006. Hyaluronate fragments reverse skin atrophy by a CD44-dependent mechanism. PLoS Med. 3, e493.
Khamanga, S.M., Walker, R.B., 2012. In vitro dissolution kinetics of captopril from microspheres manufactured by solvent evaporation. Dissolut. Technol. 19, 42–51.
Kovács, A., Zsikó, S., Falusi, F., Csányi, E., Budai-Szűcs, M., Csóka, I., Berkó, S., 2021. Comparison of synthetic membranes to heat-separated human epidermis in skin permeation studies in vitro. Pharmaceutics 13, 2106.
Kowalczyk, A., Oelschlaeger, C., Willenbacher, N., 2015. Visualization of micro-scale inhomogeneities in acrylic thickener solutions: A multiple particle tracking study. Polymer 58, 170–179.
Lau, W.M., Ng, K.W., Sakenyte, K., Heard, C.M., 2012. Distribution of esterase activity in porcine ear skin, and the effects of freezing and heat separation. Int. J. Pharm. 433, 10–15.
Lee, D., Gutowski, I.A., Bailey, A.E., Rubatat, L., de Bruyn, J.R., Frisken, B.J., 2011. Investigating the microstructure of a yield-stress fluid by light scattering. Phys. Rev. E 83, 031401.
Li, Y., Rodrigues, J., Tomás, H., 2012. Injectable and biodegradable hydrogels: gelation, biodegradation and biomedical applications. Chem. Soc. Rev. 41, 2193–2221.
Lombardo, D., Kiselev, M.A., Magazù, S., Calandra, P., 2015. Amphiphiles self-assembly: basic concepts and future perspectives of supramolecular approaches. Advances in Condensed Matter Physics 2015 (1), 151683.
Lowes, M.A., Suárez-Fariñas, M., Krueger, J.G., 2014. Immunology of psoriasis. Annu. Rev. Immunol. 32, 227–255.
Ma, L., Dong, L., Chang, P., 2019. CD44v6 engages in colorectal cancer progression. Cell Death Dis. 10, 30.
Marquardt, Y., Fietkau, K., Baron, J.M., 2020. Biological effects of hyaluronic acid-based dermal fillers and laser therapy on human skin models. J. Drugs Dermatol. 19, 897–899.
Montanari, E., Capece, S., Di Meo, C., Meringolo, M., Coviello, T., Agostinelli, E., Matricardi, P., 2013. Hyaluronic acid nanohydrogels as a useful tool for BSAO immobilization in the treatment of melanoma cancer cells. Macromol. Biosci. 13, 1185–1194.
Montanari, E., Zoratto, N., Mosca, L., Cervoni, L., Lallana, E., Angelini, R., Matassa, R., Coviello, T., Di Meo, C., Matricardi, P., 2019. Halting hyaluronidase activity with hyaluronan-based nanohydrogels: development of versatile injectable formulations. Carbohydr. Polym. 221, 209–220.
Montanari, E., Mancini, P., Galli, F., Varani, M., Santino, I., Coviello, T., Mosca, L., Matricardi, P., Rancan, F., Di Meo, C., 2020. Biodistribution and intracellular localization of hyaluronan and its nanogels. A strategy to target intracellular S. aureus in persistent skin infections. J Control Release 326, 1–12.
Montenegro, L., Parenti, C., Turnaturi, R., Pasquinucci, L., 2017. Resveratrol-loaded lipid nanocarriers: correlation between in vitro occlusion factor and in vivo skin hydrating effect. Pharmaceutics 9, 58.
Neupane, R., Boddu, S.H.S., Renukuntla, J., Babu, R.J., Tiwari, A.K., 2020. Alternatives to biological skin in permeation studies: current trends and possibilities. Pharmaceutics 12, 152.
Oppong, F.K., Rubatat, L., Frisken, B.J., Bailey, A.E., De Bruyn, J.R., 2006. Microrheology and structure of a yield-stress polymer gel. Phys. Rev. E 73, 041405.
Orsmond, A., Bereza-Malcolm, L., Lynch, T., March, L., Xue, M., 2021. Skin barrier dysregulation in psoriasis. Int. J. Mol. Sci. 22, 10841.
Pandey, S.S., Maulvi, F.A., Patel, P.S., Shukla, M.R., Shah, K.M., Gupta, A.R., Joshi, S.V., Shah, D.O., 2020. Cyclosporine laden tailored microemulsion-gel depot for effective treatment of psoriasis: in vitro and in vivo studies. Colloids Surf. B Biointerfaces 186, 110681.
Panonnummal, R., Jayakumar, R., Sabitha, M., 2017. Comparative anti-psoriatic efficacy studies of clobetasol loaded chitin nanogel and marketed cream. Eur. J. Pharm. Sci. 96, 193–206.
Panonnummal, R., Sabitha, M., 2018. Anti-psoriatic and toxicity evaluation of methotrexate loaded chitin nanogel in imiquimod induced mice model. Int. J. Biol. Macromol. 110, 245–258.
Parisi, R., Iskandar, I.Y.K., Kontopantelis, E., Augustin, M., Griffiths, C.E.M., Ashcroft, D. M., 2020. National, regional, and worldwide epidemiology of psoriasis: systematic analysis and modelling study. BMJ (Clinical Research Ed.) 369, m1590.
Rapalli, V.K., Sharma, S., Roy, A., Alexander, A., Singhvi, G., 2021. Solid lipid nanocarriers embedded hydrogel for topical delivery of apremilast: In-vitro, ex-vivo, dermatopharmacokinetic and anti-psoriatic evaluation. J. Drug Delivery Sci. Technol. 63, 102442.
Rendon, A., Schäkel, K., 2019. Psoriasis pathogenesis and treatment. Int. J. Mol. Sci. 20, 1475.
Ruwizhi, N., Aderibigbe, B.A., 2020. The efficacy of cholesterol-based carriers in drug delivery. Molecules (basel, Switzerland) 25, 4330.
Sawyer, L.M., Wonderling, D., Jackson, K., Murphy, R., Samarasekera, E.J., Smith, C.H., 2015. Biological therapies for the treatment of severe psoriasis in patients with previous exposure to biological therapy: a cost-effectiveness analysis. Pharmacoeconomics 33, 163–177.
Shah, P.P., Desai, P.R., Patel, A.R., Singh, M.S., 2012. Skin permeating nanogel for the cutaneous co-delivery of two anti-inflammatory drugs. Biomaterials 33, 1607–1617.
Shalaby, R.A., El-Gazayerly, O., Abdallah, M., 2022. Cubosomal betamethasone-salicylic acid nano drug delivery system for enhanced management of scalp psoriasis. Int. J. Nanomed. 17, 1659–1677.
Tsuji, G., Yamamura, K., Kawamura, K., Kido-Nakahara, M., Ito, T., Nakahara, T., 2023. Regulatory mechanism of the IL-33–IL-37 axis via aryl hydrocarbon receptor in atopic dermatitis and psoriasis. Int. J. Mol. Sci. 24, 14633.
Vincent, N., Ramya, D.D., Vedha, H.B., 2014. Progress in psoriasis therapy via novel drug delivery systems. Dermatol. Reports 6, 5451.

Visconti, B., Paolino, G., Carotti, S., Pendolino, A., Morini, S., Richetta, A., Calvieri, S., 2015. Immunohistochemical expression of VDR is associated with reduced integrity of tight junction complex in psoriatic skin. J. Eur. Acad. Dermatol. Venereol. 29, 2038–2042.

Waghule, T., Rapalli, V.K., Singhvi, G., Gorantla, S., Khosa, A., Dubey, S.K., Saha, R.N., 2021. Design of temozolomide-loaded proliposomes and lipid crystal nanoparticles with industrial feasible approaches: comparative assessment of drug loading, entrapment efficiency, and stability at plasma pH. J. Liposome Res. 31, 158–168.

Wang, L., Ma, X., Pan, Y., Ye, H., Liu, Z., Kuang, Z., Zhao, Z., Liu, A., Ji, Y., 2024. HA-based pH-responsive calcium ions and crocetin releasing hydrogel for accelerating skin wound healing. Chemistry–an Asian Journal e202400198.

Xu, M., Lu, H., Lee, Y.-H., Wu, Y., Liu, K., Shi, Y., An, H., Zhang, J., Wang, X., Lai, Y., 2018. An interleukin-25-mediated autoregulatory circuit in keratinocytes plays a pivotal role in psoriatic skin inflammation. Immunity 48 (787–798), e784.

Ying, L.Q., Misran, M., 2017. Rheological and physicochemical characterization of alpha-tocopherol loaded lipid nanoparticles in thermoresponsive gel for topical application. Mal J Fund Appl Sci 13, 248–252.

Zeng, F., Chen, H., Chen, L., Mao, J., Cai, S., Xiao, Y., Li, J., Shi, J., Li, B., Xu, Y., 2021. An autocrine circuit of IL-33 in keratinocytes is involved in the progression of psoriasis. J. Invest. Dermatol. 141, 596–606.e7.

Zhang, Y., Xia, Q., Li, Y., He, Z., Li, Z., Guo, T., Wu, Z., Feng, N., 2019. CD44 assists the topical anti-psoriatic efficacy of curcumin-loaded hyaluronan-modified ethosomes: A new strategy for clustering drug in inflammatory skin. Theranostics 9, 48.

Zheng, Y., Ouyang, W.Q., Wei, Y.P., Syed, S.F., Hao, C.S., Wang, B.Z., Shang, Y.H., 2016. Effects of Carbopol(®) 934 proportion on nanoemulsion gel for topical and transdermal drug delivery: a skin permeation study. Int. J. Nanomed. 11, 5971–5987.

Zhu, Q., Jiang, M., Liu, Q., Yan, S., Feng, L., Lan, Y., Shan, G., Xue, W., Guo, R., 2018. Enhanced healing activity of burn wound infection by a dextran-HA hydrogel enriched with sanguinarine. Biomater. Sci. 6, 2472–2486.

Zoratto, N., Forcina, L., Matassa, R., Mosca, L., Familiari, G., Musarò, A., Mattei, M., Coviello, T., Di Meo, C., Matricardi, P., 2021a. Hyaluronan-cholesterol nanogels for the enhancement of the ocular delivery of therapeutics. Pharmaceutics 13, 1781.

Zoratto, N., Montanari, E., Viola, M., Wang, J., Coviello, T., Di Meo, C., Matricardi, P., 2021b. Strategies to load therapeutics into polysaccharide-based nanogels with a focus on microfluidics: A review. Carbohydr. Polym. 266, 118119.

Zsikó, S., Csányi, E., Kovács, A., Budai-Szűcs, M., Gácsi, A., Berkó, S., 2019. Methods to evaluate skin penetration in vitro. Sci. Pharm. 87, 19.